Master of Science in Mechanical Engineering
May 2026

Topology Optimization as Design Support for Temporary Cable Support Holder

Cable Management During Transport within Production Facility

Tobias Johansson

Faculty of Engineering, Blekinge Institute of Technology, 371 79 Karlskrona, Sweden

This thesis is submitted to the Faculty of Engineering at Blekinge Institute of Technology in partial fulfillment of the requirements for the degree of Master of Science in Mechanical Engineering. The thesis is equivalent to 20 weeks of full-time studies.

The authors declare that they are the sole authors of this thesis and that they have not used any sources other than those listed in the bibliography and identified as references. They further declare that they have not submitted this thesis to any other institution to obtain a degree.

Contact Information:
Author:
Tobias Johansson
E-mail: jtobias@live.se

University advisor:
Ph.D. William Cockayne
Department of Mechanical Engineering

Faculty of Engineering
Blekinge Institute of Technology
SE–371 79 Karlskrona, Sweden

Internet : www.bth.se
Phone : +46 455 38 50 00
Fax : +46 455 38 50 57

Abstract

This thesis addresses the issue of transporting cables attached to a pump throughout the manufacturing process, from assembly to painting and packaging, with a solution suitable for a wide range of pumps with alternating sizes, shapes, weights, and suspension systems. In order to generate a fully functional cable carrier solution, the necessary steps of the product realization process will be included in the thesis, from idea to a manufactured prototype. To achieve a satisfying solution, multiple factors will be considered to fulfill Xylem's demands, for instance, weight, simplicity, cost, design of manufacture and generalization, where one cable carrier should be used for all pumps in the same department. To meet the demands, topology optimization will be the primary tool in this thesis, along with design science research and different concept generation methods, depending on the component of the solution. The final theoretical concept weighs just over 5 kg, mainly consisting of rectangular hollow sections with different attachments and various angles for mounting the cable holder onto the lifting bracket. The computational simulations and analytical calculations account for forces in both the horizontal and vertical directions. The difference between the finite element analysis and the analytical results is negligible, with the largest stress differences in the vertical direction. In the vertical case, peak stresses occur in the simulation model, with surrounding stresses similar to those in the analytical results. To realize the final concept, some adjustments were made to the prototype model, resulting in a total weight of 7.6 kg and satisfactory stresses in both vertical and horizontal directions. The iterative process of topology optimization in this thesis revealed that, in structural engineering, solutions often tend toward traditional geometric solutions. While topology optimization has the potential to generate complex, weight-reduced shapes, the results of this study consistently pointed toward the efficiency of the rectangular hollow section. This convergence validates that traditional profiles are not merely conventions but are mathematically reliable structures for handling multidirectional loads. Ultimately, the most successful design is not the one that removes the most material, but the one that provides the highest structural safety and operational simplicity at the lowest total cost. To summarize, the design process, in the end, comes down to cost, manufacturability, and overall profitability.

Keywords: Cable carrier, Design Optimization, Finite Element Method, Concept Generation, Topology Optimization

Sammanfattning

Denna avhandling behandlar problemet med att transportera redan anslutna kablar på pumpar genom hela tillverkningsprocessen, det vill säga från montering till målning och paketering, med ett brett produktsortiment av pumpar med varierande storlekar, former, vikter och upphängningssystem. På grund av att en helt fungerande kabelbärarlösning kommer att tas fram, kommer majoriteten av produktframtagningsprocessen att inkluderas i avhandlingen, det vill säga från idé till en tillverkad prototyp. För att kunna uppnå en tillfredsställande lösning kommer flera faktorer att beaktas för att uppfylla Xylems behov, det vill säga vikt, enkelhet, kostnad, tillverkningsdesign och generaliserbarhet, då kabelbäraren ska kunna användas för alla pumpar inom samma kategori. För att uppnå dessa krav kommer topologioptimering att vara det primära verktyget, tillsammans med designvetenskaplig forskning och olika metoder för konceptgenerering. Det slutliga teoretiska konceptet hade en slutvikt på drygt 5 kg, huvudsakligen av rektangulära ihåliga rör och en konsol med olika spår med olika vinklar för att kunna montera kabelbäraren på lyftfästet på pumpen. Beräkningssimuleringarna och de analytical beräkningarna beaktade krafter både horisontellt och vertikalt. Den finita elementanalysen och de analytiska resultaten har försumbara maximala spänningsskillnaden, medan den horisontella riktningen har orealistiska toppspänningar i simuleringsmodellen, men med liknande omgivande spänningar som de analytiska resultaten. För att kunna realisera det slutliga konceptet till en prototyp behövdes några justeringar genomföras, vilket resulterade i en totalvikt på 7,6 kg och spänningar med god säkerhetsmarginal både vertikalt och horisontellt. Den iterativa processen för topologioptimering i denna avhandling gav insikt att beräkningsoptimering ofta konvergerar mot traditionella geometriska lösningar. Även om topologioptimering har potential att generera komplexa viktreducerade former, pekade resultaten i denna studie konsekvent mot fördelarna med den rektangulära ihåliga profilen. Denna konvergens bekräftar att traditionella profiler inte bara är konventioner utan matematiskt tillförlitliga strukturer för att hantera laster i flera riktningar. I slutändan är den mest framgångsrika designen inte den som tar bort mest material, utan den som ger högst strukturella prestanda och enkelhet till lägsta totalkostnad. Sammanfattningsvis handlar designprocessen i slutändan om kostnad, tillverkningsbarhet och övergripande lönsamhet.

Nyckelord: Design Optimering, Finita Elementmetoden, Kabelkrok, Konceptgenerering, Topologioptimering

Acknowledgments

Hereby, I want to acknowledge my gratitude towards the excellent collaboration and support I got from my supervisor Andreas Björnsson, employees at the construction department: Madeleine Hermann, Henric Dackling, Magnus Amnér and the employees of the project department at Xylem Water Solutions AB in Emmaboda, in order to complete this thesis.

I also want to express my appreciation towards my supervisor William Cockayne at Blekinge Institute of Technology, for his good insights and highly skilled expertise throughout the thesis project.

Sincerely, Tobias.

Contents

List of Figures

List of Tables

List of acronyms

BC Boundary Condition

CAD Computer Aided Design

CAE Computer Aided Engineering

CF Constraint Function

DSR Design Science Research

FEA Finite Element Analysis

FEM Finite Element Method

FE Finite Element

OF Objective Function

PTC Parametric Technology Corporation

RHS Rectangular Hollow Sections

SIMP Solid Isotropic Material with Penalization

TO Topology Optimization

List of Symbols

Symbol	Description	SI-Unit
E	Young's modulus	Pascal [Pa]
N_i	Shape function	-
u_h	Trial function	-
a_i	unknown constant	-
ρ_i	density element	-
$f(x), G(x), V(x), H(x)$	objective functions	-
x	Design Variable	-
n_x	Number of design variables	-
$g(x), h(x)$	Constrain functions	-
a, b	Constants	-
i, j, l	Index range	-
p	penalization power	-
d	Distance	[m]
h, H	Height	[m]
b, B	Width	[m]
t	Thickness	[m]
I	Second Moment of Inertia	$[m^4]$
δ	Deflection	[m]
σ	Stress	[Pa]
e	Distance from starting axis to edge	[m]
L	Length	[m]
a	Distribution of load	[m]
q	Distribution of load	[m]
c	Unloaded distance	[m]
N	normal force	Newton [N]
v, φ	angle	[degrees]
D	Diameter of rolled cable	[m]
M	Moment	[m]
A	Area	Square Meters $[m^2]$
F	Force	Newton [N]
P	Pressure	Pascal [Pa]
σ	Stress	Pascal [Pa]
z	prescribed displacement	[m]

Chapter 1

Introduction

The transportation of a diverse product range often presents significant logistical challenges in manufacturing environments. These operations require frequent, inefficient tool changes, disrupting production flow and increasing operational costs. This thesis addresses the issue of transporting pumps from a testing rig to a painting facility. The flow has a wide range of product sizes, shapes, weights, and suspension systems. The pumps require a power supply to provide sufficient electrical power to pump water. Since pumps vary widely in purpose, the cables differ in size and weight to meet each pump's specific electrical needs, resulting in differences in length and diameter. The cable is mounted to the pump before testing and must follow the pump through the entire manufacturing process, so it must be attached to the pump without disrupting processes before and after entering the painting facility, such as testing and drying. This also requires that the dimensions of the attachment solution be taken into account to fit within the various operations. The current solution for securing the cable is shown in figure 1.1, with the names of the components indicated that interact, and a total weight of 9.6 kg.

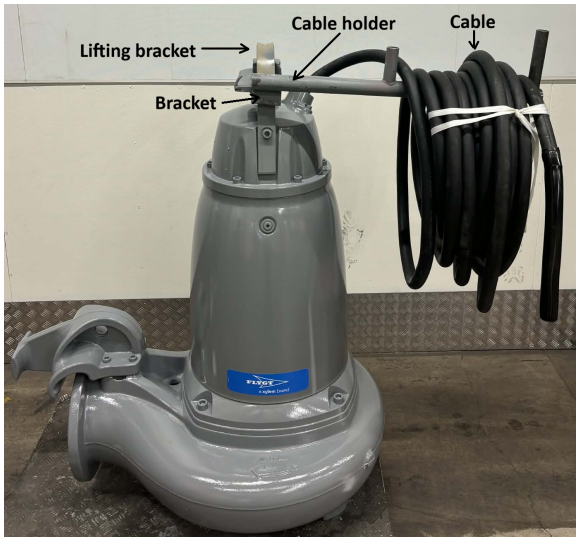

Figure 1.1: The previous solution of the cable holder.

The attachment solution for attaching the cable to the pump must be efficient and easy to use to reduce production costs and increase the flow of goods. The current solution at the company for this operation consists of various cable holders for different lifting brackets and cables. With the weight of the cable holders varying

from 4 to 9.6 kg.

Cables are flexible, which leads to alternating placement and often uneven placement toward the center of mass. Furthermore, during application, the cable may be placed more inaccurately by the operator, leading to oscillations during application and transport. Load variations introduce uncertainty in the parameters governing the structure's behavior, which needs to be investigated. To design a solution that satisfies all uncertain boundaries, a generalized solution must be obtained. This study is of public interest to various actors in the transport and industrial sectors, who need to transport cargo using hooks or attachment solutions to secure it, especially when the distribution of forces varies and is uncertain. Through simple benchmarking, a common problem in an industrial environment could be identified.

It is a customer demand that the cable attachment system is to be generalized to fit a wide range of products, to make it more cost-effective, and preferably make it so cheap that it could be shipped to the customer. If a low-cost cable hook solution is feasible, a complex version will be produced first by TO. Furthermore, the cable holder needs to secure the cable safely, and both the cable and the cable holder need to be easy to lift off. Additionally, the cable holder needs to have a low weight, to make it easier for the operator to deal with, while still fulfilling manufacturability through design of manufacture, and thus make the solution cost-efficient.

Furthermore, the attachment systems must withstand the alternating loads from a wide range of cables, making durability and strength the primary design considerations. This thesis will use TO on the system to meet all customer demands, to find a suitable and functional concept.

1.1 Problem Statement

Computational methods can be used in all kinds of scenarios. One important genre is the transport sector. More precisely, the transportation of goods in different facilities between operations. The most common modes of transport are conveyor systems and trucks, depending on demand, for instance, overhead or roller conveyor systems. In order to use this transportation safely, it is required to develop a cable holder to secure additional cargo during transport. This operation needs to be time-efficient and safe for the operator to perform. Furthermore, the cable carrier needs to withstand cargo loads from a strength and durability perspective. In manufacturing industries, it is common to use a variety of different sorts of lifting hooks, where the solutions are different depending mainly on geometry and weight. These systems do not often have a clear solution and must be adjusted depending on the operations performed across the different facilities. The uncertainty could lead to trade-offs, making the solution less optimal for certain customer demands, for instance, increased weight to withstand a certain load or increased weight due to manufacturability and cost efficiency.

In this case, pumps will be transported from a testing rig to a painting facility, with a wide range of pumps with alternating sizes, shapes and weights. The pumps require different sizes and weights of cables, which differ in length and diameter. The cables need to be attached to the pump without disturbing processes before and after entering the painting facility, such as testing and drying.

The management of the cable holder for attaching the cable to the pump must be efficient to reduce production costs and increase the flow of goods. The current solution at the company for this operation consists of various kinds of cable holders for different lifting brackets and cables. It is suitable that the cable holder is as generalized as possible to fit a wide range of products, to make it more cost-effective. First, a requirement spec needs to be constructed to meet all the customers' demands, where different parameters will have different priorities. Then TO will be performed to find a suitable solution, where requirement conflicts will occur and trade-offs will be necessary. Lastly, utilize the design of manufacture with consideration of the trade-offs. Further, the cable holder needs to withstand the alternating loads from the wide range of cables, which makes durability and strength the most important factors to consider. Where topology optimization must be performed on the system to optimize the concept.

1.1.1 Aim and purpose

The aim of the thesis is to design, analyze and optimize a cable carrier for the cargo to transport additional equipment, by applying TO with FEA. The goal is to improve structural performance, increase reliability, reduce weight, and minimize material consumption, since multiple cable holders need to be produced to meet the production rate of goods entering the painting facility.

1.1.2 Delimitations

This thesis will focus solely on cable carriers in industrial manufacturing and on their effects on geometry under different operating conditions.

The design of the concepts is focused on functionality, weight reduction and manufacturability. Since the cable holder will be produced in large quantities, economic efficiency will be considered to maintain manufacturability. A simple version would yield economic benefits, where water cutting could be a cost-effective alternative.

The structural analysis will consist of a static linear elastic study, where only the parameters of the critical cable will be used as inputs to the TO process to ensure the structural integrity of the cable holder. In the concept generation phase, all cable dimensions will be considered to meet the cable carrier's requirements. Furthermore, the dimensions of the different manufacturing processes will be considered to ensure that the system of both the pump and cable holder fits within the whole manufacturing process. Lastly, the solution will be translated into a physical prototype to assess its reliability and compliance with requirements for future mass production.

1.1.3 Research objectives and hypotheses

The current cable holder solution implemented in the manufacturing process has two issues. Firstly, different cable hooks are required for different pumps, which increases

costs and storage space. Secondly, the increased weight due to the over-sizing of the current solution is also a concern because of the system's sensitivity to tilt during transport while standing or hanging in a conveyor system. From an ergonomic point of view, when mounting the cable holder. To solve this problem, a new cable holder will be designed and developed as a weight-optimized replacement for the current solution. The thesis will answer the following research questions:

- What is the optimized geometry of the lifting solution using topology optimization, considering minimizing the Von Mises stresses and material consumption under different loads?
- How can results from topology optimization be used to develop a solution that considers different types of cargo?

The thesis has the following hypothesis:

- The most exposed parts, where critical stresses occurs needs more material. In regions with negligible stress, the material distribution will be reduced.
- The design of the attachment solution will include additional material at approximately the same locations for different loads. The noticeable difference should be in the amount of material required to apply.

1.1.4 Thesis Outline

The thesis consists of a frame of reference, which provides the theoretical background and related research in order to get a fundamental knowledge base to be able to implement the necessary tools to solve the problem statement. Then comes the method, which describes the different tools utilized in the work process and how to ensure validity and reliability. The next chapter describes the practical work progress and implementation of the chosen methods, including the course of action of the concept generation, evaluation, design optimization and TO phase. Then the results and analysis of the work process are presented, including the final solution, the design of manufacture with the corresponding FEA simulation and the validation of the analytical calculations. The physical prototype is also presented in the results, along with its corresponding analytical calculations. The following chapter discusses the takeaways from the concept generation phase and the design- and TO phases, and how the work contributes to the research on industrial manufacturing. The last chapter presents a conclusion based on the discussion and identifies parts of the work that could be investigated further to achieve a more robust and optimized solution.

1.2 Ethical, societal and sustainability aspects

Optimized products using TO avoid over-dimensioning and reduce material consumption, resulting in less material waste and lower material costs. If a generalization is possible and weight reduction could bring economical benefits, since it is cheaper to buy larger batches of the same product and lowers the material costs. If the solution fits more products, it reduces confusion when selecting the correct cable carrier

during cable attachment, thereby lowering production cycle times and potentially reducing stoppages, thereby increasing profit. The reduced risk of confusion when fewer cable holders are available also improves operator safety, since selecting the wrong cable holder could result in its failure, leading to injuries.

Chapter 2

Frame of reference

This chapter provides a theoretical background on the theory and prior research to achieve the intended purpose of this thesis.

2.1 Theoretical background

This section describes the intended theoretical approaches and methods used in the practical work of the thesis. Mainly consisting of the FE computational method and the TO procedure.

2.1.1 Finite Element Analysis

Finite Element Analysis FEA is based on FEM implemented into computer aided engineering Computer Aided Engineering (CAE) software. This is used to predict and analyze a system's behavior, thereby avoiding computationally expensive calculations and enabling the software to perform the calculations [1]. The mathematical model is not ideal and needs to be adjusted for each situation. The model is also dependent on the accuracy of the mesh, where a finer mesh that includes more differential equations tends to converge the results to the ideal theoretical solution [2]. The accuracy gained from a finer mesh comes at the cost of reduced computational efficiency. Therefore, when using FEA, there is a constant trade-off between accuracy and computational time. In order to tackle this problem, an irregular mesh could be used, where a finer mesh could be applied in domains of interest and areas with less criticality could have a coarser mesh.

2.1.1.1 Finite Element Method

The Finite Element Method FEM starts with defining the governing differential equation for the problem, also called the strong form [2]. The strong form is then transformed into the so-called weak form, which makes it possible to use polynomial functions to find a solution. The transformation is done by multiplying the differential equation by an arbitrary test function and integrating over the solution domain, which is achieved by integration by parts to reduce the order of the derivatives. FEM then divides the entire solution domain into smaller sub-domains called elements, which are surrounded by nodes. To approximate the solution within these elements, shape functions (N_i) are used. The approximate solution, also called the

trial function (u_h), is the sum of the shape functions multiplied by unknown nodal constants (a_i) defined as:

$$u_h = \sum_i a_i N_i \tag{2.1}$$

Lastly, the trial function (u_h) and the boundary conditions are substituted into the Weak Form, which has now transformed the continuous integral problem into a discrete system of linear equations.

2.1.2 Structural Optimization

Optimization within design is an iterative process that often has multiple requirements that need to be met simultaneously [3]. The user is required to intervene at each iteration until a final design solution is obtained. To avoid manual labor, certain optimization strategies can be applied, which makes the iterative process automatic while still meeting the users' requirements of the design. In the design, structural optimization methods could be divided into shape-, size-, and topology optimization. The shape optimization involves modifications to the appearance in the form of material distribution, while improving or maintaining performance. Size optimization adjusts cross-sectional dimensions while maintaining the functionality of the structure. Topology optimization investigates the material distribution and geometry within the given design space.

2.1.2.1 Topology optimization

TO is an iterative process used in order to determine the optimal design [4], with given boundary conditions, constraints and loads. In this case, this is done by changing the geometry based on stress analysis. If it occurs critical stresses on the model, adding material is an option, while in parts with low stresses, the material could be reduced. Then the simulation is remade to analyze the new changes, which is done until the user reaches satisfaction.

The first component to take into consideration is the material distribution. That is a discrete function from 0 to 1, where 0 means no material absence and 1 indicates full presence of material [5].

$$\rho_i \in \{0, 1\} \tag{2.2}$$

In TO, the distribution of material is the OF $G(\rho_i)$, so this function will either be minimized or maximized. The function G can, for instance, be stress or volume and can be written as:

$$G = G(\rho_i) = \int_\Omega g(\rho_i) dV \tag{2.3}$$

The Objective Function (OF) now needs to take the constraints into consideration while the function is being optimized. Since TO is an iterative process, one important constraint is that the current iterated volume does not exceed the original volume:

$$H_0(\rho_i) = \int_\Omega \rho_i dV - V_0 \leq 0 \tag{2.4}$$

Where the TO can have multiple constrains descried as:

$$H_j(\rho_i) \leq 0, \quad j = 1, ..., m \tag{2.5}$$

Where m is the number of constrains.

The selection of Objective Functions OF and Constraint Functions Constraint Function (CF) is a critical decision in structural topology optimization. As discussed in the comprehensive review by Sigmund and Maute [6], the most common formulation is maximizing stiffness, subject to a predefined volume fraction constraint. However, a significant issue arises when parameters are predetermined. A strict volume constraint gives a lightweight structure, but could at the same time result in a geometry that fails to meet the required stiffness.

Sigmund and Maute highlight that while density-based methods are computationally efficient for these formulations, the physical feasibility of the result is highly dependent on the initial boundary conditions and constraint values. To address the difficulty of estimating these values in practical engineering, the optimization process in this study follows an iterative approach. By factoring in both weight reduction and stress limits, the design is refined to ensure that the final cable carrier achieves weight reduction without compromising the structural integrity required for the cable cargo.

2.1.2.2 Design variables

Design variables are used to describe the system and can be expressed as a column vector:

$$x = [x_1, x_2, ..., x_{n_x}] \tag{2.6}$$

The variables describe the design and n_x is the number of design variables in the system that determines the dimensionality of the problem. The parameters in the vector must be independent to avoid infinite combinations of vectors with the same value, which results in an infinite number of combinations of values corresponding to the same design [3].

2.1.2.3 Objective- and Constraint functions

An objective function OF is a mathematical expression used to determine whether the current design is more optimal in a given situation than the previous design [3]. The OF can be maximized or minimized depending on the user's demand, where weight or volume is often used OFs.

The design space in the OF defines the domain where the design variables are allowed to change. The space is defined by constraint functions CF, which are mathematical functions defining bounds and controlling the optimization procedure.

The given OF is then optimized by finding the minimum or maximum local value called the optima within the domain of the OF. The following statement describes the minimization of the OF within the design variables and given bounds, subjected to the constraints.

$$\begin{array}{lll} \text{minimize} & f(x) & \\ \text{by varying} & a \leq x_i \leq b & i = 1, \ldots, n_x \\ \text{subject to} & g_j(x) \leq 0 & j = 1, \ldots, n_g \\ & h_l(x) = 0 & l = 1, \ldots, n_h. \end{array} \tag{2.7}$$

Where $f(x)$ is the OF that needs to be optimized, the design variable x_i is subjected to the domain a and b, and $g_j(x)$ and $h_l(x)$ are the CFs. It should be noted that all the functions can assume any mathematical shape, for instance, discrete or continuous functions. These statements are essential for selecting the most appropriate optimization algorithm. The suitability of a specific algorithm depends on the mathematical properties of the OFs and CFs, specifically their linearity and the availability of gradients. However, practical applications often rely on FEM solvers, which output discrete numerical datasets rather than analytical expressions. Consequently, the reliance on FEM imposes constraints on algorithm selection, as methods requiring analytical gradients may not be applicable.

2.2 Related Work

This part explores existing literature regarding lifting equipment design, structural analysis and the application of TO. It summarizes relevant studies to establish a theoretical background and identifies the research gap regarding a generalized attachment solution for alternating loads.

2.2.1 Hook Design Loading by The optimization Method With Weighted Factors Rating Method

In "Hook Design Loading by The optimization Method With Weighted Factors Rating Method" by A. Manee-ngam, P. Saisirirat, and P. Suwankan, they investigated how a 2-ton lifting hook can be designed with respect to cost, strength, security, and aesthetics [7]. This was done by using "the optimal designed method" together with "the highest weight method".

By applying ISO 7597 (forged steel lifting hooks with latch of grade 8) standards and FEA, the authors identified a hook model superior to standard designs, achieving a reduction in production material costs of 27.49 % and an increase in safety factor by 42.16%. Their hook was also lighter than standard hooks. The study concludes that this optimization method successfully defines dimensions for a superior prototype suitable for future development. This thesis focuses on optimizing a similar solution regarding weight reduction, maximizing performance and cost-effectiveness.

2.2.2 A topology optimization design of a crane hook

In the article "A topology optimization design of a crane hook" by Vu Duc Hiep, Nguyen Xuan Quynh and Tran Thanh Tung, they investigated the effectiveness of topology optimization techniques applied to ABS plastic. The primary objective was

to reduce weight while maintaining structural durability for a crane hook prototype [8].

The researchers analyzed stress distributions and optimized the design within the material strength limits of a 3D model of a current existing hook. The specific constraints for their study were a maximum material usage of 1 kg ABS plastic and a target lifting capacity of 5 kg.

The analysis concentrated on ensuring that stress levels remained within the material's strength limits, and the research proposed five different models that satisfied these requirements. It provided an indication that this method is economically efficient and optimizes both material and time.

This article uses the intended methodology of TO, thus following a similar approach as intended in this thesis.

2.2.3 Stress constrained topology optimization

In the paper "Stress constrained topology optimization", Erik Holmberg, Bo Torstenfelt and Anders Klarbring developed and evaluated a method for handling stress constraints within TO [9]. Their objective was to minimize mass or maximize stiffness while addressing the computational cost.

The authors utilized a clustering technique to group the stress evaluation points using a modified P-norm.

They provided a detailed sensitivity analysis applicable by both 2D- and 3D structures. The numerical validation was performed with 2D bilinear quadrilateral elements.

Their stress-constrained formulation provided significantly different topologies compared with traditional stiffness-based formulations. Their approach successfully avoided stress concentrations that other methods often fail to resolve. The investigation uses the TO methodology for an L-shaped beam structure, which has a structural appearance similar to that of the intended lifting solution. This gives an indication of the probability of the stress and material distribution that the lifting solution will encounter during simulation.

2.2.4 Topology optimization and fatigue analysis of lifting hook

In the article "Topology optimization and fatigue analysis of lifting hook" by Ibrahim T. Teke, Mustafa Akbulut and Ahmet H. Ertas redesigned a lifting hook using topology optimization combined with fatigue analysis [10]. The method in this study was density-based in order to minimize volume. To achieve this, the FEM is used in a commercial software, where a standard lifting hook was remodeled using Computer Aided Design (CAD) software. After the TO, the new model obtained was analyzed; this procedure was repeated three times for each different model. The conclusion of the study says that it is possible to reduce the weight of a lifting hook while still obtaining the required strength. This study is an iterative TO procedure for optimizing a lifting equipment solution, which is a similar methodology to that described in this thesis.

2.2.5 Thesis relation to the Related work

From a general perspective, this thesis investigates the implementation of TO in the design of industrial components that are exposed to multi-axial loading and dynamic constraints. To explore its potential for industrial scalability and resource efficiency. This thesis will contribute a methodology for handling complex boundary conditions under uncertainty. Since traditional optimization often assumes fixed load points. The investigation will examine how to effectively discretize continuous moving loads and varying contact interfaces into a robust set of load cases. The aim of this investigation is to produce a guideline for how to design attachment solutions where the exact load application point is a variable or unknown, while still considering minimizing weight, manufactureability, maximizing stiffness and cost efficiency.

Chapter 3

Method

3.1 Research method

In this thesis, Design Science Research DSR is utilized as research method.

3.1.1 Design Science Research

Design science consists of the scientific study and creation of artifacts that are used to solve practical problems [11]. The method is based on practical problems from a problem-solving standpoint for solving them. This consists of creating, positioning and repurposing the artifacts that are possible solutions to the problem. Furthermore, design science is an empirical study that generates new knowledge through direct observation, experience or experimentation based on primary data for explication and evaluation.
However, Design science and design need clarification to avoid misunderstanding, as they are very similar to each other in definition. The difference lies in their purposes, with their generalization and contributions to knowledge differing. Design Science requires that the results produce knowledge of general interest, whereas causal design provides knowledge benefits only to a single client, and the newly extracted knowledge cannot be used by other actors.
There are three characteristics to extinguish them both. Firstly, Design Science projects are required to use rigorous research methods, in order to obtain new knowledge of general interest. Moreover, the newly extracted knowledge needs to be related to a current knowledge bank to ensure a reliable knowledge foundation for the obtained results. Lastly, the newly obtained knowledge needs to be distributed to the practitioners and the research community.
The practical problem of general interest for this thesis is a non generalized and heavy cable carrier that requires multiple tools for different products. The artifact in this scenario will be a weight-optimized cable carrier to solve the practical problem. The research is carried out using the commonly used computational methods, TO and FEM. Furthermore, the design will be based on already existing methodologies and algorithms. This thesis will also be published in a public forum and shared with Xylem Water Solutions Manufacturing AB.

3.1.2 Method framework

Firstly, the problem needs to be identified and have a clear motivation. Define the required objectives that the solution needs to achieve [12]. It is now time for the design and development phase. When the concept is complete, it needs verification in the form of a demonstration, in this case is a simulation. Lastly, the final solution needs evaluation to confirm that the objectives are fulfilled. Finally, the solution needs to be shared with its stakeholders and other relevant contributors within the same research area.

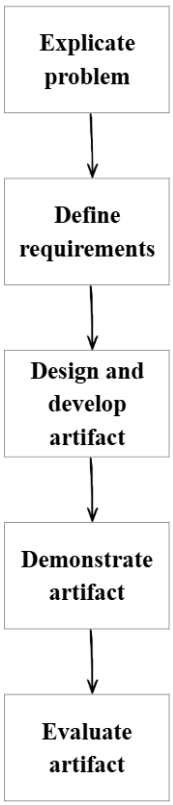

Figure 3.1: DSR framework.

[11]

3.2 Concept generation

3.2.1 Heuristic approach

The aim of the Heuristic approach is not to find the ideal solution, rather to find a satisfactory or suboptimal solution based on the constraints and circumstances [13, 14] This method does most of the time obtain satisfying results, but sometimes inaccurate answers may occur. The beneficial part of the heuristic algorithms is that they have a reasonable execution time, on the other hand, it cannot always be proven that the solution is a globally optimal solution.

In a search for a suboptimal design, heuristics act as a ranking method used at every branching step [15]. Instead of testing every possible geometric variation, the developer uses available information to decide which design path or branch to follow and which to discard.

The heuristic process works through a systematic elimination of candidates. Firstly, the identification of all potential concepts is treated as "candidates" for the final solution. Then, each concept is ranked and filtered, with each candidate evaluated against specific rules, such as accessibility, stability, and manufacturing cost. Furthermore, if a candidate fails a primary condition, e.g., if the contact surface is too small or the manufacturing cost is too high, that "branch" is discarded. Lastly, the iteration restarts with the next-closest candidate until a solution is found that satisfies all functional requirements.

In this thesis, the transition among six concepts was performed as a heuristic search. Each failed iteration provided new information that updated the "rules" for the next branch, eventually allowing the search to converge on a final, functional design without the need for exhaustive, infinite testing.

3.2.2 Empirical Research

Empirical research is a study where conclusions are derived exclusively from concrete, verifiable evidence rather than theoretical speculation [16]. This methodology is grounded in the principle that knowledge is obtained through the direct observation and measurement of real-world phenomena. In the context of this project, the empirical method was used to replace manual procedures with scientific experimentation to determine a suitable arm length of the cable holder without having knowledge of the center of gravity of the pumps.

3.2.3 Multi-Critera Decision Making

Multi-criteria decision-making is a structured decision-support system used to evaluate scenarios where multiple, often conflicting, dimensions must be captured simultaneously [13]. In the context of TO, these dimensions typically include volume, mass, Von Mises stresses, manufacturing feasibility, and total cost.

The decision-making process mirrors aspiration-level models, which compare various design iterations against an ideal solution. Since the constraints in TO are often in direct conflict, such as the trade-off between minimizing material volume and maintaining structural stiffness. The framework is used to identify the alternative that is closest to the desired aspiration level.

To ensure the results are robust and acceptable, it is essential to avoid black-box models, as they are difficult to understand for the decision makers. Instead, a transparent approach is more beneficial to use, where the weighting of criteria, such as prioritizing manufacturing simplicity over marginal weight savings, is clearly defined. This ensures that the final suboptimal results are more acceptable and easier for the decision maker to grasp.

3.3 Approach of Topology Optimization

3.3.1 Software

The construction work to create the 3D-models and simulations of the cable carrier solution was performed in Parametric Technology Corporation (PTC) Creo CAD software. The software has an Finite Element (FE) simulation tool to perform the FEA, which is a vital tool in order to perform the TO. Furthermore, does Creo have a built-in generative design tool, which enables automatically driven simulations where an optimal geometrical shape is generated based on the user's demands and constraints.

3.3.2 Density approach

Sigmund and Maute conducted an extensive review of various solution frameworks, specifically comparing the "density," "level set," "topological derivative," and "phase field" methods [6]. Their analysis concluded that the differences in computational efficiency among these approaches are often negligible and highly dependent on the specific implementation. Given the lack of a single "fastest" method, the density-based approach is adopted in this thesis due to its high degree of industrial maturity and integration into automated mechanical design environments. The density method operates by allowing the material distribution variable ρ_i, to take continuous values between 0 and 1. While a discrete search for the optimal shape would be computationally exhaustive, the transition to a continuous function enables the use of gradient-based optimization. By ensuring the objective function is differentiable, the optimal material distribution can be efficiently calculated. To ensure a physically meaningful result, the Solid Isotropic Material with Penalization (SIMP) method is utilized to penalize intermediate densities, effectively "pushing" the solution toward a binary state of either solid material or void.

3.3.3 Solid Isotropic Material with Penalization

The Solid Isotropic Material with Penalization SIMP method is a material distribution approach where the design domain is discretized into finite elements [5]. Each element i is assigned a relative density variable, ρ_i, which can vary continuously between 0 representing a void and 1 representing solid material. The core of the SIMP method is the power-law relationship used to determine the Young's Modulus (E) of each element based on its local density:

$$E_i(\rho_i) = \rho_i^p E_0 \tag{3.1}$$

Where:

ρ_i is the relative density of the element ($0 \leq \rho_i \leq 1$).

E_0 is the Young's Modulus of the fully solid material.

p is the penalization power (typically $p = 3$).

Aurora emphasizes that without a penalization factor ($p > 1$), the optimization process would result in regions with intermediate densities that are physically impossible to manufacture. By setting $p = 3$, the stiffness-to-weight efficiency of intermediate densities is reduced. This disproportionately low stiffness for intermediate values pressures the optimization algorithm to push the densities toward the binary extremes of 0 or 1, ensuring a more manufacturable result.

3.4 Validation and Reliability

To ensure the scientific integrity of the results, specific measures were taken to address the validity and reliability of the simulation and optimization process. In this context, validity refers to the accuracy with which the model represents the physical behavior of the cable holder, while reliability concerns the consistency and repeatability of the numerical results.

3.4.1 Model Simplification and Symmetry

To increase the validity of the study, the simulation model was strategically simplified. A key decision was the application of symmetry Boundary Conditions Boundary Condition (BC)s, allowing for the analysis of only half of the cable carrier. This approach significantly reduces the total number of degrees of freedom in the FEM solver. By reducing the computational load, it was possible to allocate more resources to a higher polynomial order within the remaining elements, thereby increasing the precision of the stress results without exceeding realistic computational time, resulting in an increase in TO iterations. This trade-off between model size and numerical depth is a critical factor in ensuring that the results are not subject to discretization errors.

3.4.2 Convergence Method

In the FE simulation the multi pass adaptive convergence method is used in the Creo simulate function [17]. The method performs multiple solutions steps by increasing the polynomial order for every iteration and locally refining mesh areas with high strain energy until the given convergence percent of the overall local strain energy is fulfilled [18, 19]. For every time the polynomial level is increased, the total degrees of freedom will also increase in the model [20]. Checks will then be performed locally in the area where changes in strain energy and displacement are the greatest. The polynomial level is then increased in those areas and the simulation will be performed again. This process will then be performed iteratively until the results converge, so if the results change by less than the given percent, the algorithm will stop.

3.4.3 Boundary Conditions and Constraints

The placement of constraints and loads was iteratively validated to ensure high internal validity. In the early stages of the study, hand calculations were performed to estimate the expected reaction forces and maximum bending moments of the carrier

under its self-weight and cable load. These analytical results were used to verify that the constraints in PTC Creo were correctly placed. By comparing the hand calculations with the preliminary FEA results, it was confirmed that the model investigated the intended mechanical phenomena. If the boundary condition is placed close to sharp corners and next to load-bearing parts, the simulation gives significantly inaccurate stresses. The constraints were placed at the root of the arm seen in figure 3.2.

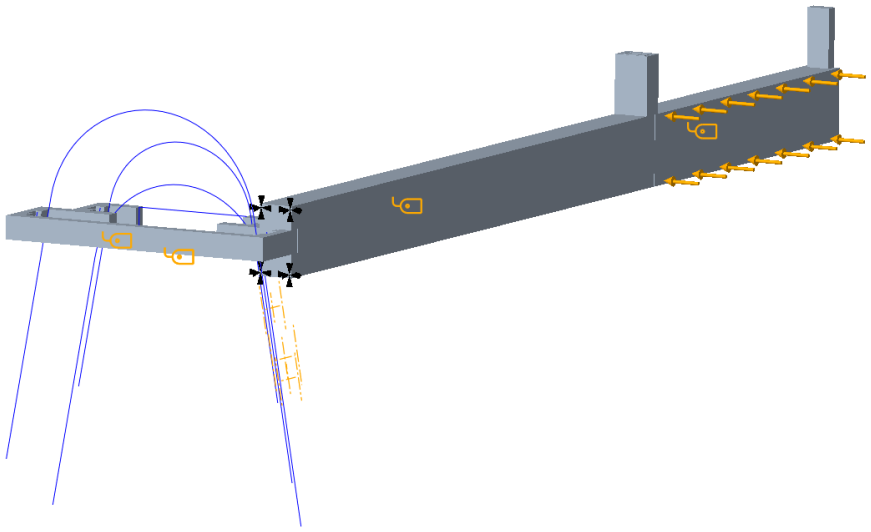

Figure 3.2: Placement of constrains at the root of the arm visualized as black crosses.

Chapter 4

Implementation process

To achieve this, the first objective is to design a concept and build a numerical model of the cable carrier using the finite element method. When the numerical model is implemented, it will be possible to identify critical points, as well as the deformations and behavior of the system under load. Furthermore, simulations are required to investigate how design parameters affect performance, such as geometry, material properties and the placement of supports. When the testing is complete, it is possible to optimize the design with respect to weight, stiffness and strength. For instance, to reduce material consumption while obtaining a robust solution. At last, evaluate the results and either repeat the iteration to obtain more satisfactory results or directly draw conclusions for future designs of cable carriers for transporting heavy and alternating loads.

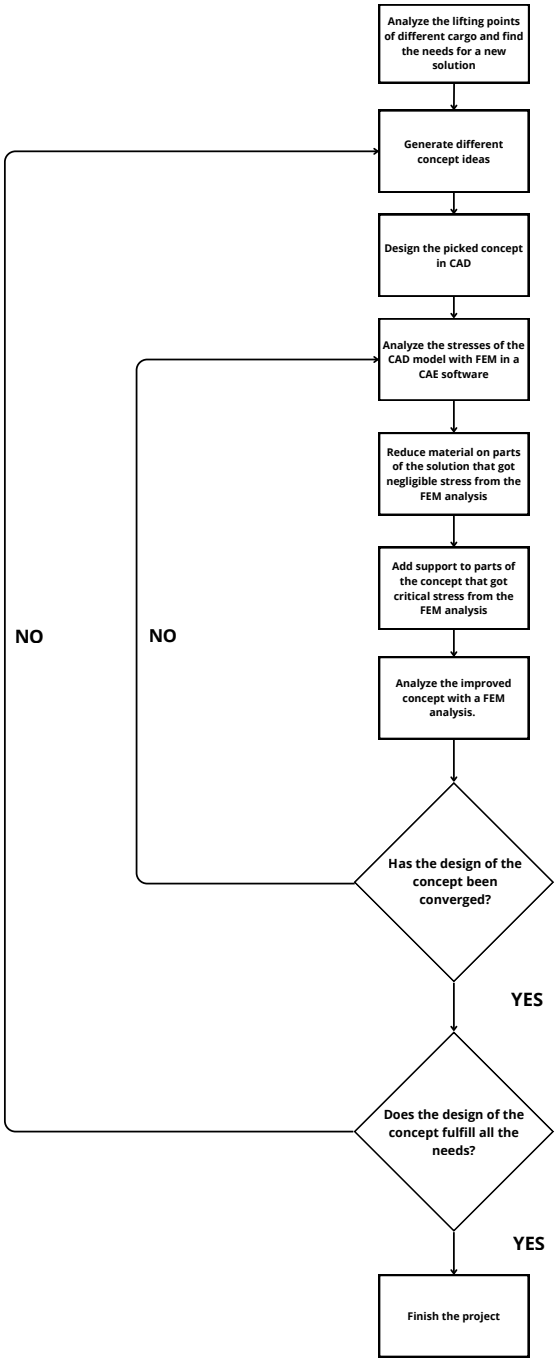

Figure 4.1: Flow chart of the process of solving the problem.

4.1 Requirement specification

The requirements of the solution are determined in consultation with the project department, where the different parameters were ranked based on the manufacturing processes and economic factors in the following order.

- Cost efficiency & Manufacturability
- Generalization

- Minimizing of weight

Note that, since manufacturability is connected to cost efficiency, a simpler solution to manufacture gives a lower cost per unit, and they are both considered equals.

4.2 Concept generation and evaluation

This section will describe the concept generation process and evaluation in order to find a suitable solution.

4.2.1 Concept generation for attachment solution for bracket

The concept generation phase was conducted first through brainstorming and then by visualizing the different concepts. In order to find the best solution, trial and error were conducted. For every iteration, some new knowledge about the requirements could be obtained, which finally resulted in a fully functional solution that fulfilled all the requirements.

The initial idea was to find a common measure with a common denominator, since they all shared a similar geometry. In order to mount the attachment from above A.1, as in the previous solution. This idea was quickly ruled out because the bracket width varied widely, making it impossible to find a common approach. The second idea, shown in figure A.2, was to use the attachment above to find a common measure at the top of the lifting brackets. However, limited access when hooking up the pump and an unstable solution since there is a low contact surface for the different lifting brackets. The third idea shown in figure A.3 was to rotate the second concept ninety degrees vertically to improve access. This idea failed during testing of the 3D-printed version because the generalization limited the contact surface between the geometries and was nonexistent for the smaller brackets seen in figure A.4. The pump is also tilted in the testing facility, increasing the risk that the attachment solution glides out of the lifting bracket. The fourth idea shown in figure A.5 was to have different tracks for the different lifting brackets in order to increase the contact surfaces. This solution was clumsy, reduced access for hooking the pump and a confusing attribute for the operator when mounting the cable hook seen in A.6. The fifth concept seen in A.7 was to use the similarities from above, as that had the most common measurements among all the lifting brackets. This solution is at high risk of tilting under the cable load shown in figure A.8. Due to its complex geometry, it will be difficult to manufacture and then costly. It also has limited access to hooking the pump. The sixth solution shown in figure A.9 involved finding similarities between some of the lifting brackets. This resulted in two of three having an acceptable attachment solution, which provided two adjacent forms for inserting the lifting bracket with a stabilizer with an offset from the bracket shown in figure A.10, to provide sufficient access when hooking the pump. When 3D-printing an actual prototype of the sixth concept and then testing it on the lifting brackets, there was excess space, so the stabilizer could be reduced until the final concept A.11.

4.2.2 Determination of arm length

Multiple criteria need to be fulfilled in order to achieve a satisfactory arm length of the cable holder. First, it needs to fit through the entire process after mounting, from testing to painting, with sufficient access for the robot to paint the pump while the cable is attached. The cable holder also needs to meet specific dimensions in the testing facility due to the geometry of the testing equipment. Lastly, the moment created by the arm length and cable can cause the pump to overturn when placed on the ground or to tilt while hanging in a traverse system. The painting robot requires 300 mm of free space to perform the painting. The distance from the lifting bracket to the edge of the pool is 1330 millimeters in the big pool and 670 millimeters in the smallest pool. In order to find a satisfactory arm length, experiments were performed, where the smallest pump model and the biggest model were tested on how much cable they could carry until too much tilt was obtained and when they overturned.

The first experiment consisted of applying as much cable as possible to the smallest pump to make it overturn, where a 100 kg cable could be applied 200 millimeters from the bracket before overturn.

Figure 4.2: Experimental setup of the first experiment.

Figure 4.3: Applied cable load at pump stationed at the solid ground.

Figure 4.4: Weighting of cable to ensure its actual weight.

The second experiment was conducted in order to gain knowledge of the moment needed to tilt the pump while hanging in the traverser system using the smallest model.

Figure 4.5: Experimental setup with a 100 kg cable loaded onto the cable hook.

Figure 4.6: 40 kg cable loaded onto the cable hook while in air.

The third experiment included both overturning and tilting in the air, based on the largest model.

Figure 4.7: Experimental setup of the biggest pump with an applied load 270 kg cable while stationed at the ground.

Figure 4.8: Experimental setup of a 270 kg loaded cable while the system is hooked to the conveyor system.

Figure 4.9: Unloading cable until no tilting at all while the pump is hooked to the conveyor system.

Based on this data, a suitable arm length could be obtained by using the moment equation. From the third experiment, a 170 kg cable could be placed 54 cm away from the pump with a satisfying tilt while hanging in the traverse system. The multiplication of those two is 9210 $kg \cdot cm$. If a center of gravity is chosen at 65 cm, all criteria are fulfilled, which gives an ordinary equation of:

$$d \cdot 65 = 9210 \Rightarrow d = 140kg \tag{4.1}$$

The pump tested is not the heaviest, so those pumps will often not have a cable weighing over 140 kg. This concludes that the placement of the center of gravity is satisfactory. We also need the cable to extract at least 30 cm from the pump to get enough access for robot painting, which gives the following properties of the arm length:

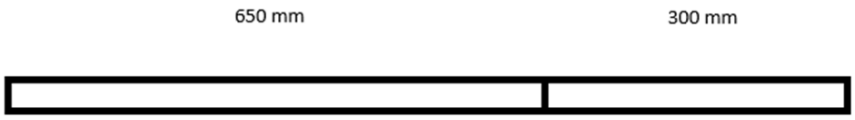

Figure 4.10: Overview of the needed estimated arm length in order to have no tilting while the pump is connected to the conveyor system.

The 650 mm arm is the original arm that will be mounted to the attachment, and the 300 mm arm will be removable to accommodate the smaller pumps in the testing facility.

4.2.3 Concept generation for arm

The requirement for the cable holder is that the cable should be easy to attach and detach with another hook before entering the painting facility. This requirement means that the cable must have free access at the top to avoid oscillations during the hooking of the cable from the cable holder, which could cause injury to workers or damage to goods. The initial concept was either a fork solution with two arms that provide sufficient space to hook the cable or a basket solution consisting of a crescent. Since the different cables have varying dimensions in all directions, a basket solution is challenging to meet all requirements while still providing easy access when hooking the cable. The basket solution will also result in irregular cable placement within the basket, which can make it difficult to hook the cable in some cases, whereas two arms will provide consistent placement and access at all times. For the fork solution, two initial concepts were created, one with just two arms both mounted to the attachment solution and the other with one arm mounted either at the middle or at the side and then two arms further out, as seen in figure 4.11.

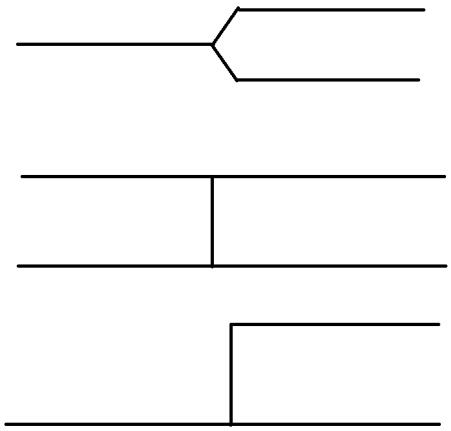

Figure 4.11: Initial concept ideas of the design of the cable arms.

With the arm in the middle, it will be too difficult to hook the lifting bracket for the smallest pump due to limited access in that region, and the arm will clash with the cable connector. One arm will also provide less robustness and a weaker solution due to many turns, which are critical points in a structure.

With the two arm solution, another complication will arise. Since the cable is circular, it will create an inward force because the normal force is perpendicular to the contact surface, which is, in this case, not vertical and at an angle, as seen in figure 5.14. In order to reduce weight, the initial solution was to have a small width of the arms and have a support in between the arms. This support was needed to be placed far out on the structure to provide sufficient support and avoid failure, which would otherwise make it too difficult to hook the cable. To increase the space to hook the cable, a U- or V-shaped solution was studied, but was declined quickly due to high material consumption of the V-shape and weak structure due to the multiple turns creating the U. In order to solve this, a wider arm structure is necessary. To avoid increasing material requirements, a hollow profile is needed, either circular as before or rectangular. After the simulation, the rectangular solution gave higher structural performance and lower material usage. Lastly, to make the cable holder suit all operations, a modular arm solution with two arm lengths was developed. Since the different sizes of the pumps have different testing facilities, which have different dimensions. For the smaller pump, the arms mounted to the attachment are used and for the bigger pump with more cable, an additional arm is mounted at the tip of the original arm.

4.3 Design- and Topology Optimization

This section describes the iterative process for finding the optimal cable holder solution based on TO. The results are based on the worst-case scenario, where two 100 kg cables are distributed across the entire 600 mm cargo area. Since there are no standard cable sizes and weights, the only way to ensure the hook's strength is to design the structure based on the heaviest cable case. Due to symmetry, only

one arm is considered in the simulation to reduce computational time and increase accuracy, which leaves the model to consider only a 100 kg cable distributed over the entire cargo area.

4.3.1 Initial concept

The initial concept had beams as arms with a uniform rectangular cross-section, as seen in figure 4.12. As expected, the highest stresses occurred at the root, corresponding to the maximum bending moment in that position.

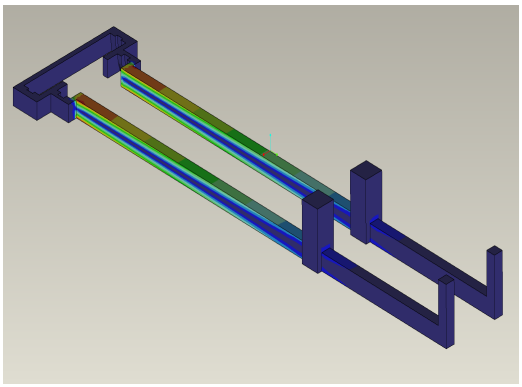

Figure 4.12: FEA of the initial concept with uniform rectangular arms. Severe stress concentrations are visible at the root due to the maximum bending moment.

In figures 4.13 and 4.14, iterative modifications were evaluated by increasing the height distribution along the arm while maintaining the same width as the base in figure 4.12. This suggests that the structure's height is the most critical parameter for achieving increased strength while maintaining low weight.

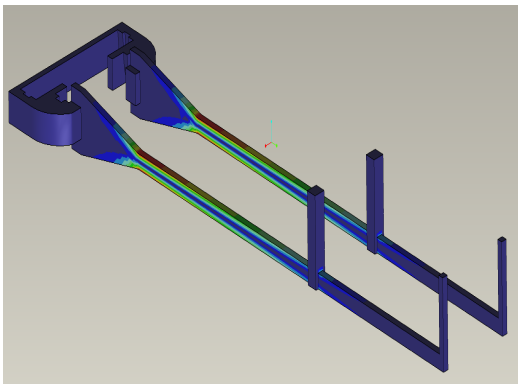

Figure 4.13: First iteration of evaluating the increased height at the base. The stress concentration shifts outward along the arm.

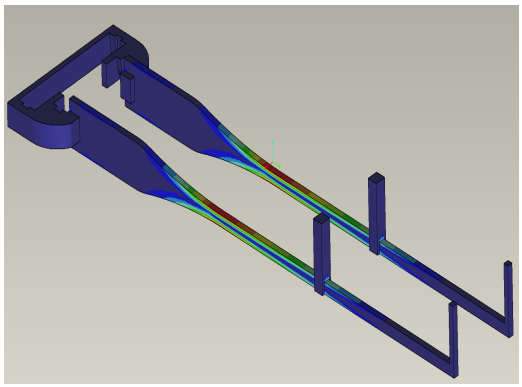

Figure 4.14: Second iteration with further increased distribution of the same height, with the same structural inefficiency.

Figure 4.15 displays a solution with satisfactory stress concentrations at the expense of increased material distribution. Instead of expanding the width, the vertical height of the arms was increased at the root, creating a tapered profile.

Since the beam's second moment of inertia and the corresponding bending stiffness are proportional to the cube of its height, this modification efficiently handles the bending moment in the root. This results in significantly decreased stress along the arm with the increased height, while the root, which is the critical part of the arm remains within safe stress limits. Now the stress concentrations move to the link between the arm and the modular arm, which has the same cross-section as before. Since the bending moment decreases due to the shorter lever arm, the stresses in the link end up within safe margins.

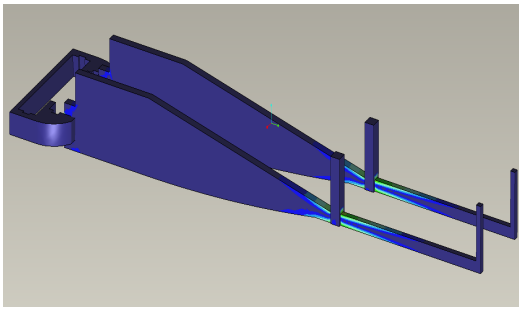

Figure 4.15: Solution with increased vertical height at the arm, which reduces the stresses.

4.3.2 Second concept

Continuing with the iterative TO of the beam's height and width to further refine the design. The primary objective of this process was to minimize the overall mass of the arms while preserving structural stiffness and loading capacity by adjusting the structure's height and width. By defining the allowable design space for the tapered arms through iterative removal of material from regions experiencing negligible stress. The optimization reduces the width and gives a tapered appearance. This process generated a geometry similar to an I-beam, where the optimization maximized the second moment of inertia, while reducing the structure's weight. The figures from 4.16 through 4.23 illustrate the iterative material reduction and the final interpreted geometry.

Figures 4.16 and 4.17 introduce the initial phase of the TO. Figure 4.16 establishes the maximum allowable design space from the profile developed in the previous step. In Figure 4.17 width and height reductions are made to find the geometrical limits.

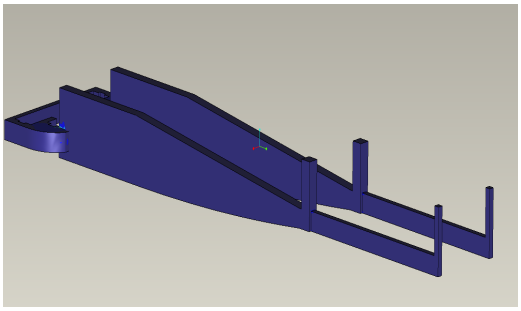

Figure 4.16: The initial design from the first iteration of the TO, before material reduction.

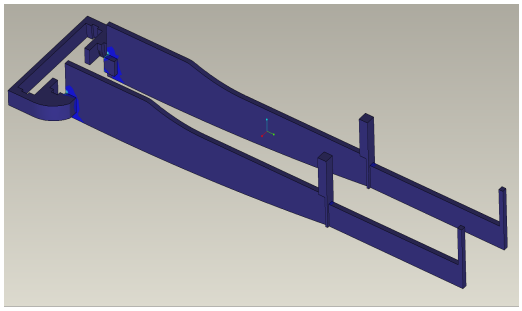

Figure 4.17: First iteration with a slight reduction of height and width of the arms.

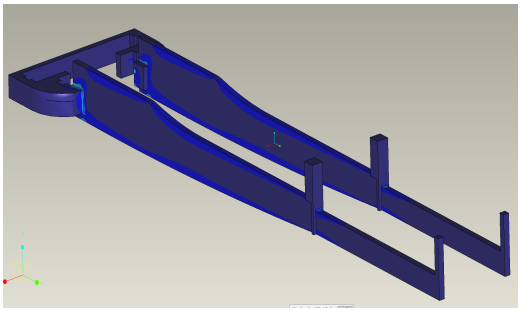

Figure 4.18: Reducing of height of the arm to find a suitable height, while still maintain a satisfactory strength.

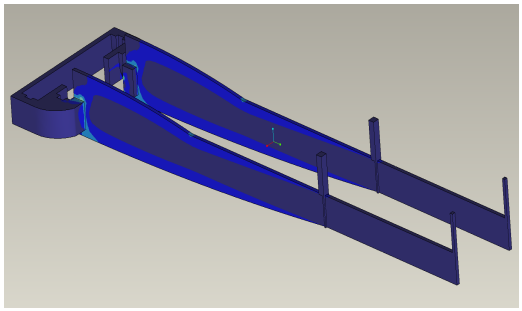

Figure 4.19: Width reduction, removing sharp corner and modular arm with the same height at as the arm.

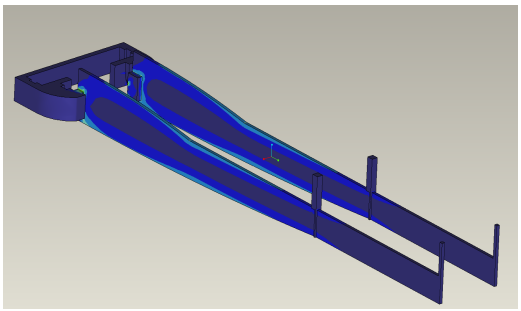

Figure 4.20: Further testing of geometrical parameters, adjusting the shaped on the top of the arm.

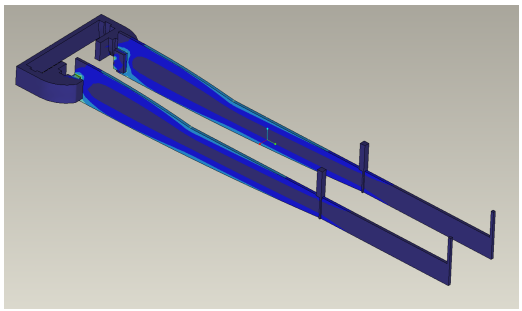

Figure 4.21: Further testing of geometrical parameters to meet stress requirements.

Figures 4.18 to 4.21 illustrate the progressive hollowing of the structure. As the width is reduced in the arms, an I-beam shape begins to emerge. This behavior aligns with beam bending theory, where normal stresses are minimal at the center and maximal at the top, creating tension, whereas the lower part experiences maximal compression. The central material and width are structurally redundant and can be removed to reduce weight, whereas the height is the primary parameter for structural integrity.

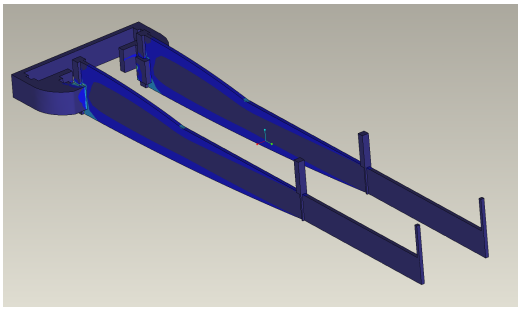

Figure 4.22: Increased width of the arm at the merge, due to critical stresses in the region.

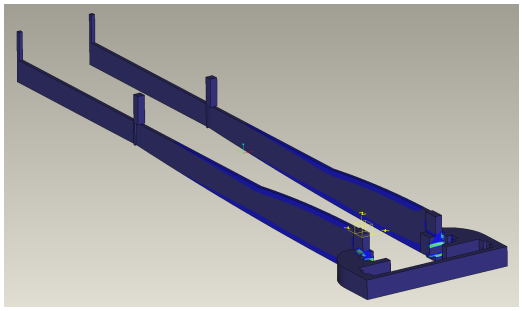

Figure 4.23: Reduced height of the attachment bracket in order to further reduce the weight of the structure.

Figures 4.22 and 4.23 have a final arm width of 5 millimeters. Compared with 20 millimeters at the beginning, it has a significantly reduced width. The increased width in the arm at the merge also provided more space to reduce the weight from the attachment, due to the decreased stresses in the merge region.

Hence, the sequence of Figures 4.16 through 4.23 demonstrates the iterative process of removing non-critical mass from the structure. The iterative optimization targets the material placed along the beam's width.

This behavior perfectly aligns with Euler-Bernoulli beam theory, during bending, normal stresses are essentially zero at the neutral axis and reach maximum tension at the top and compression at the lower parts [21]. By systematically narrowing the sides by reducing the width, the iterative TO process produces a structure similar to an I-beam. This geometry is mathematically ideal for this specific load case, as it maintains a large second moment of inertia to resist bending, while reducing the overall weight of the component. Furthermore, the material is strategically placed where the bending moment is most critical, which is at the root of the connection between the arm and the bracket.

In the second iteration, a critical reconstruction of the solution was performed. The initial shape of figure 4.16 is manually optimized based on the applied load case. It does not account for practicality and is therefore impractical for conventional manufacturing methods, which introduce localized stress concentrations at the merge, as seen in figure 4.23. Consequently, from Figure 4.16 to Figure 4.23, the concept was reverse-engineered into a clean, parametric CAD model. This was achieved by applying smooth transitions and reduced wall thicknesses. Additionally, appropriate fillets at sharp edges. The reduced weight and increased structural integrity of the optimized design made the solution more practical and manufacturable, with a total weight of 5.96 kg.

4.3.3 Generative Topology Optimization

In the next phase, the focus shifts to Generative TO. Unlike previous iterations that primarily modified the outer boundaries or hollowed out the arms to reduce weight, the generative design algorithm is allowed to remove material freely, often resulting in complex skeletal structures. The objective of the generative TO is to explore the absolute limits of mass reduction for the arms under the established

load cases. By allowing internal cutouts, the optimization process forms a truss-like framework that theoretically maximizes the stiffness-to-weight ratio. The sequence of Figures 4.24 through 4.27 illustrates the process from raw generative data to a finalized manufacturable CAD model.

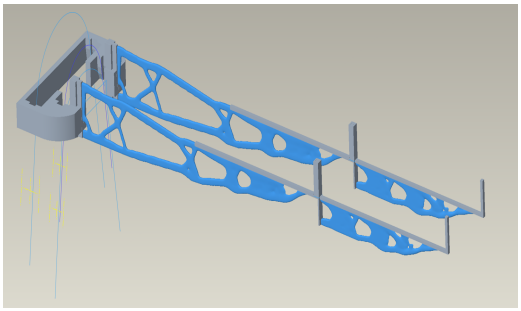

Figure 4.24: Raw output from the generative TO solver, displaying an optimized and truss-like material distribution with complex internal voids.

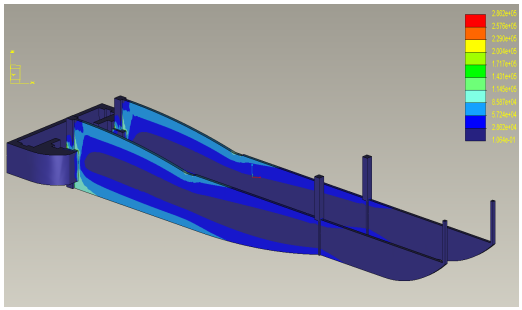

Figure 4.25: FEA of the solid profile, clearly highlighting the negligible stress regions located along the neutral axis of the beam.

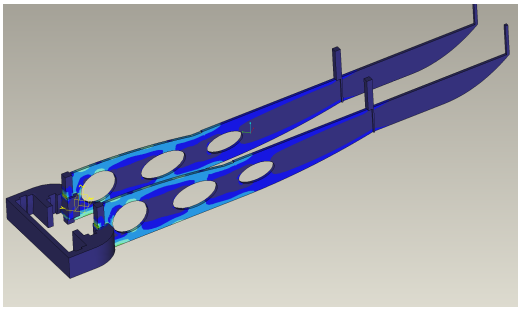

Figure 4.26: Elliptical cutouts of the solid profile have been introduced along the neutral axis, replacing the complex generative version with manufacturable features.

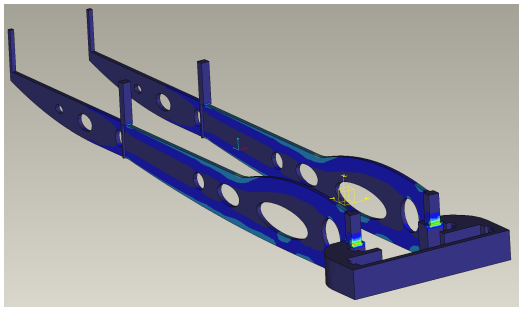

Figure 4.27: The finalized geometry with all strategically placed cutouts which mimics the generative solver's voids, reducing mass while maintaining similar stress levels.

The progression from figures 4.25, 4.26 and 4.27 illustrates the process of translating the generative design into a practical and manufacturable solution. The raw generative output in Figure 4.24 proposes a skeletal structure that represents the ideal material distribution. However, such complex geometries are often too expensive to produce using conventional manufacturing methods while still using the desired material.

To implement the generative TO into a manufacturable solution, a realistic geometry was first created and simulated in figure 4.25. This simulation provides a baseline stress analysis of a solid version, confirming that the material situated along the horizontal neutral axis experiences negligible stress. Leveraging both the traditional beam theory principle and the solution provided by the generative design in figure 4.24, the final design seen in figures 4.27 was developed. The elliptical cutouts remove structurally redundant mass and illustrate the weight-saving benefits of the

generative design, where the continuous upper and lower flanges are intentionally preserved to handle tensile and compressive stresses. The resulting stress distributions in figures 4.26 and 4.27 prove that this interpreted design successfully balances mass reduction with structural integrity and manufacturability, with a total weight of 5.26 kg, resulting in a weight reduction of 13 percent using generative TO in comparison to the solution in the second concept generation.

4.3.4 Considering forces inwards

Up to this point, the structural optimization primarily focused on maximizing bending stiffness under vertical loads from the cable. However, a complete system analysis revealed a critical secondary load case involving transverse inward forces generated by the lifting cable. The cable lies on both arms, and the circular shape of the cable creates an angular contact surface in reference to the vertical force, which results in a horizontal force component pulling the arms toward each other, as seen in figure 5.14. A free body diagram and trigonometry calculations based on two 100 kg cables resulted in an inward lateral force of 538 N, approximately equivalent to 55 kg per arm, as seen in equation (5.17). This realization created a severe structural challenge. The previously optimized solution is robust against vertical bending and its narrow width results in a low second moment of inertia in the vertical axis, making it vulnerable to lateral forces. Furthermore, the given constraint requires that the space between the arms remain completely unobstructed to allow access for the lifting hook to hook the cable. This prevented the implementation of a simple, rigid cross-member connecting the two arms to counteract the inward force in the modular part of the solution, where the critical deflection will occur. Figures 4.28 and 4.29 illustrate attempts to solve this lateral loading issue by adding support in the acceptable regions. Where the cross support solution seen in figure 4.29 is an attempt to get support closer to the critical region, in order to reduce the deflection.

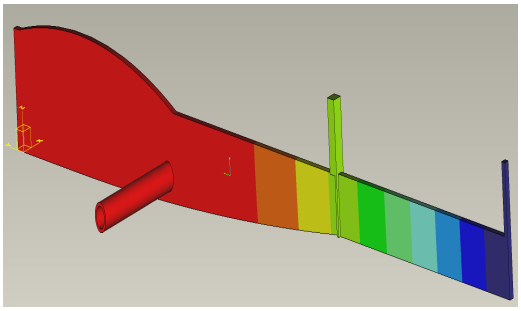

Figure 4.28: Simulation of the deflection using a pipe to counteract the horizontal forces. The analysis shows a critical lateral deflection along the thin profile due to the large bending moment in the modular part.

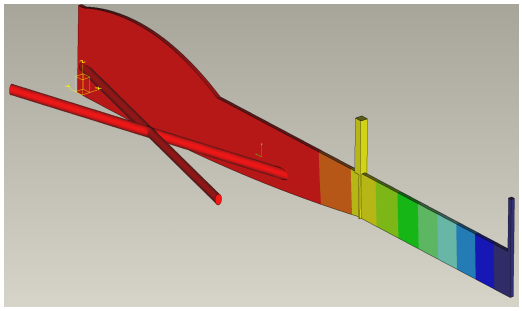

Figure 4.29: Iteration attempt to counteract the lateral forces using cross-bracing rods, where the structure still exhibits severe inward deformation due to the lack of support at the modular part.

The FEA results presented in figures 4.28 and 4.29 demonstrate the fundamental vulnerability of the thin profile arm concept when subjected to multi-axis loading.

Both iterations to support the inward forces failed to provide sufficient lateral stiffness. The simulations highlight critical transverse deformation, where the acceptable placement of the supports did not provide any noticeable difference. The strict requirement of needing access when hooking the cable prohibits a solid and continuous bridge between the two arms at the point of load application. The individual arms must bear the twisting and bending moments independently, making the structure fragile under lateral forces. The simulations confirmed that there is no geometrically feasible solution that can withstand the inward force while maintaining the required space between the arms and still have a reasonable total weight. Other concepts were considered, including V-shaped or U-shaped block solutions, which could be applied to solve the problem. However, due to manufacturing complexity and increased material use, both solutions were dismissed. This realization dictated that the independent thin arm paradigm was inadequate for the multi-axis load case, which resulted in a change in the design strategy to accommodate both the lateral cable forces and the required access for hooking the cable. Furthermore, the total weight increased to 7.0 kg to compensate for the inward forces with the cross support, which was still insufficient.

4.3.5 Rectangular- and Circular hollow pipes

Following the revelation that the independent thin-profile arms were inadequate at withstanding the inward forces generated by the lifting cable, the design strategy took a new direction. To successfully manage both the primary vertical and horizontal bending, the arms require a significant increase in their horizontal second moment of inertia. Consequently, the focus shifted from a complex iterative process to hollow pipe profiles. Hollow structural sections, particularly rectangular tubes, offer torsional rigidity and multidirectional bending strength while remaining lightweight.

The initial concept of the square solution had a total weight of 7.658 kg and is shown in figure 4.30.

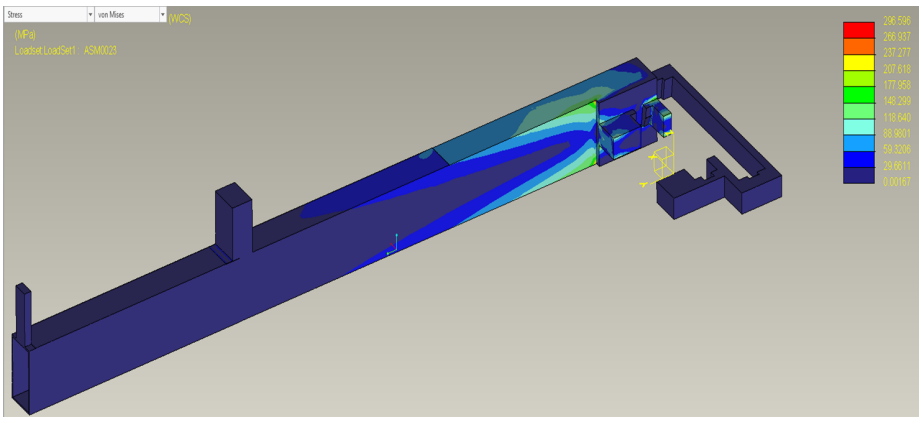

Figure 4.30: Initial conceptual solution of the rectangular hollow pipe solution.

Table 4.1: Comparison of structural performance of different beam profiles.

Parameter	**Rectangular Hollow Section**	**I-Beam**	**C-Beam**
Outer dimensions (H x W)	60 x 30 mm	60 x 30 mm	60 x 30 mm
Scenario 1: Same wall thickness			
Wall thickness (t)	1.25 mm	1.25 mm	1.25 mm
Cross-sectional area	218.75 mm^2	146.88 mm^2	146.88 mm^2
Moment of inertia (I_x)	104,333 mm^4	84,530 mm^4	84,530 mm^4
Moment of inertia (I_y)	35,348 mm^4	5,634 mm^4	13,219 mm^4
Weight of beam	**1.72 kg**	**1.15 kg**	**1.15 kg**
Result / Conclusion	*Strongest & heaviest. Highly stable.*	*33% lighter, but 19% weaker vertically.*	*Same as I-beam, but highly prone to torsion.*
SCENARIO 2: Optimized for equal vertical strength ($I_x = 104,333$ mm^4)			
Required thickness (t)	1.25 mm (Fixed)	1.57 mm	1.57 mm
Weight of beam.	1.72 kg	1.44 kg	1.44 kg
Required extra weight in mounting bracket.	(0 kg)	40x15x47 mm (0.22 kg)	40x30x47 mm (0.44 kg)
Total weigth of beam + extra material for the bracket.	**1.72 kg**	**1.66 kg**	**1.88 kg**
Final conclusion	*Excellent all-round choice for multi-axial loads.*	*Lightest overall assembly.*	*Heaviest assembly due to block volume.*

A comparative FEA study was initiated to evaluate various standard pipe geometries and wall thicknesses under the established multi-axis load cases shown in table 4.1, based on the same method as the analytical calculation in chapter 5. The objective was to identify a commercial profile that could safely handle the inward cable force and the vertical load while minimizing the overall weight. Figures 4.31 through 4.34 illustrate the stress distribution across different tested profiles.

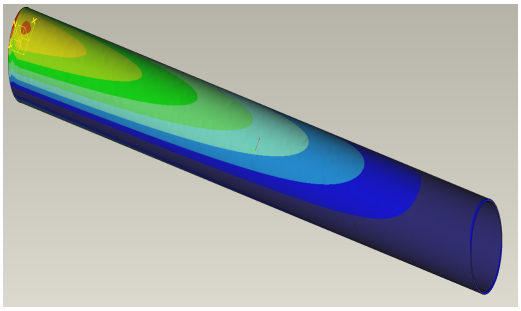

Figure 4.31: FEA of a round pipe ($60 \times 60 \times 5$ mm).

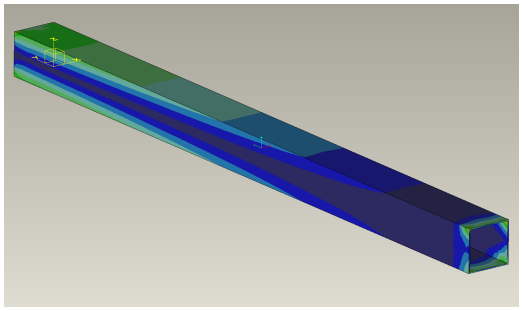

Figure 4.32: FEA of a square pipe ($60 \times 60 \times 1.4$ mm).

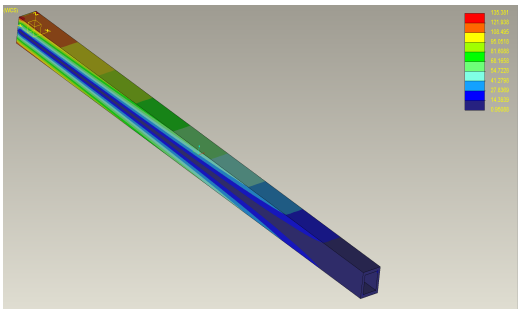

Figure 4.33: FEA of a smaller square pipe ($40 \times 40 \times 5$ mm).

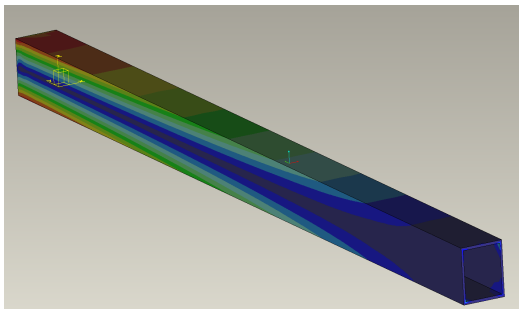

Figure 4.34: FEA of a thin-walled square pipe ($40 \times 40 \times 2$ mm).

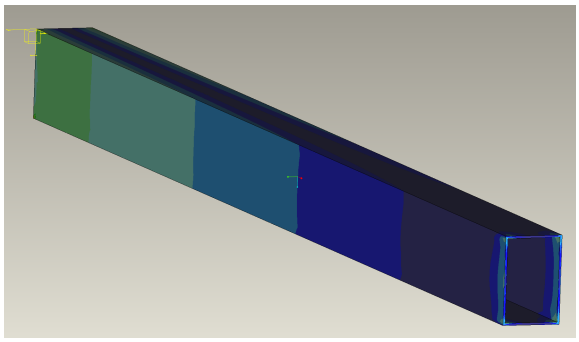

Figure 4.35: FEA of a rectangular profile ($60 \times 40 \times 1.5$ mm). The asymmetric cross-section provided strong vertical stiffness and sufficient lateral width to handle the inward forces.

The FEA simulations confirmed that Rectangular Hollow Sections (RHS) offered the best geometric compromise for the multi-axis loads. To finalize the exact dimensions and select the optimal profile, a series of manual analytical calculations was performed. Table 4.2 summarizes these calculations for three feasible rectangular profiles based on the results of the simulations, evaluating them against S235 steel with a yield strength of 235 MPa under both the vertical (100 kg) and horizontal (55 kg) load cases. The analytical summary reveals that the $60 \times 20 \times 1.5$ mm profile is dangerously close to yielding under lateral forces with a safety factor of 1.11, making it unacceptable. The $60 \times 30 \times 1.5$ mm profile offers a safety factor of 1.5, but at

Table 4.2: Summary of alternative pipe profiles and their corresponding weight of cable hook, compared to safety factor against S235: 235 MPa.

Profile (H×B×t)	**Applied force**	**Deflection (δ)**	**Max pressure (σ)**	**Safety factor**	**Status**	**Weight**
60×30×1,5 mm	From side (55 kg)	10,0 mm	127 MPa	**1,85**	Safe	5,7 kg
60×30×1,5 mm	Above (100 kg)	6,1 mm	155 MPa	**1,51**	Safe	
60×30×1,25 mm	From side (55 kg)	11,7 mm	149 MPa	**1,58**	Safe	5,2 kg
60×30×1,25 mm	Above (100 kg)	7,2 mm	184 MPa	**1,28**	Safe	
60×20×1,5 mm	From side (55 kg)	24,8 mm	211 MPa	**1,11**	Ok	4,4 kg
60×20×1,5 mm	Above (100 kg)	7,7 mm	196 MPa	**1,20**	Ok	

the cost of increased weight to 5.7 kg. Lastly, the 60 × 30 × 1.25 mm profile was selected as the final optimized solution. As demonstrated in the hand calculations, this profile safely withstands both load cases with acceptable safety margins, with safety factors of 1.45 laterally and 1.28 vertically. By reducing the wall thickness to 1.25 mm, the final design maintains structural integrity and solves the inward force issue, while achieving a satisfying overall weight of 5.2 kg. When mounting all the components together to create a more realistic model, the maximum stress created by the vertical force was 183.6 MPa and the displacement was 6.66 mm.

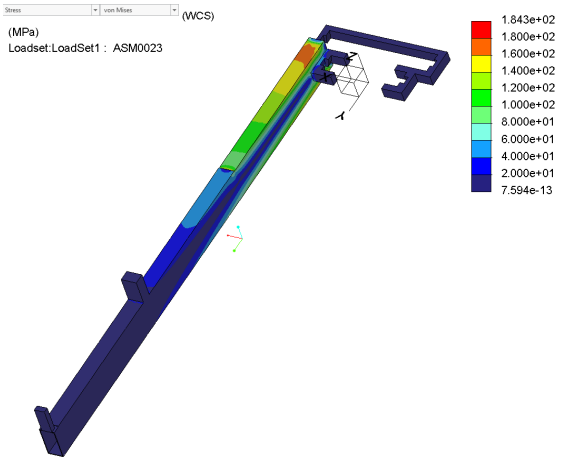

Figure 4.36: FEA assembly of a vertically force of 100 kg load with a maximum Von Mises stress of 183, 6 MPa.

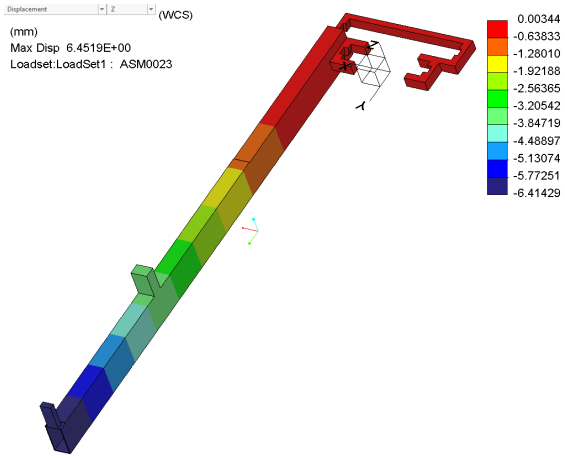

Figure 4.37: FEA assembly of a vertically force of 100 kg load with a maximum displacement of 6, 66 mm downwards.

The horizontal force produced a maximum stress of 252 MPa, due to sharp edges at the bracket. The surrounding stress lies around 150 MPa. The inward displacement 10.69 mm. The concept weighed 5.06 kg, and without the modular arms attached 3.6 kg. The arms consist of a cross-section 60x30x1.25

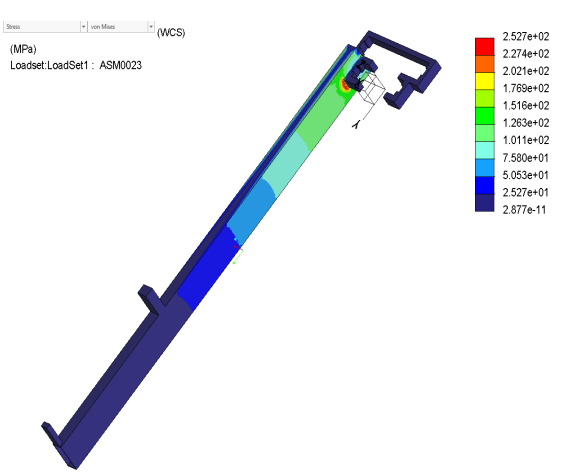

Figure 4.38: FEA assembly of a horizontally applied force of 55 kg load with a maximum Von Mises stress of 252, 7 MPa.

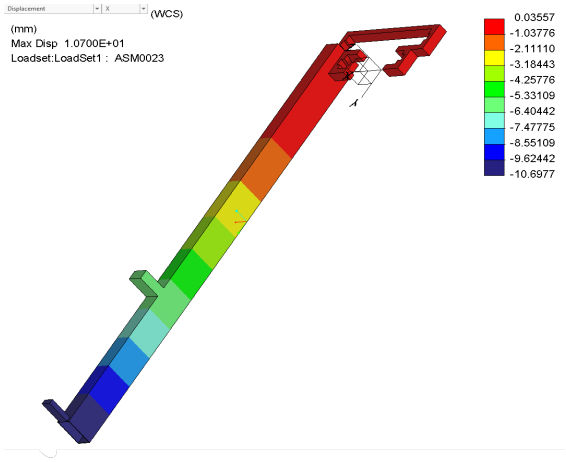

Figure 4.39: FEA assembly of a horizontally applied force of 55 kg load with a maximum displacement of 10, 69 mm inwards.

When using both the horizontal and vertical forces in the same model the stresses increased, which can be seen in figures 4.40 and 4.41.

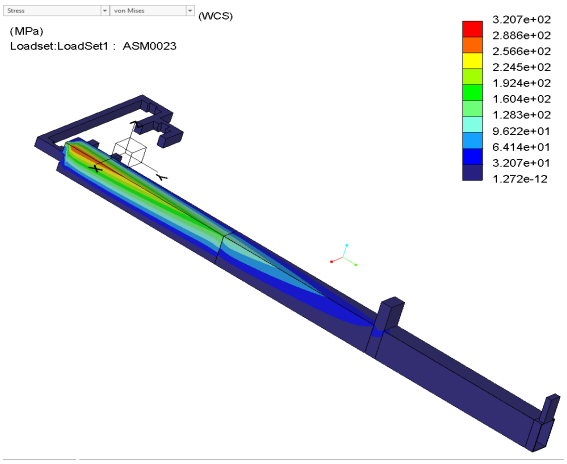

Figure 4.40: FEA assembly using both loads with a maximum Von Mises stress of 320, 7 MPa.

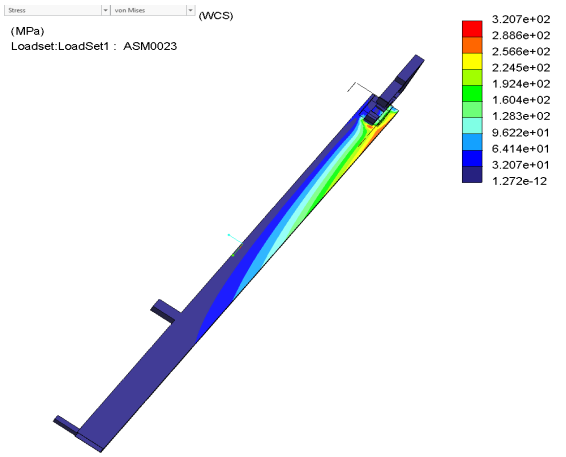

Figure 4.41: FEA assembly using both loads from the inside to show stress concentrations close to the bracket.

While the displacements remained approximately the same, which can be seen in figures 4.42 and 4.43.

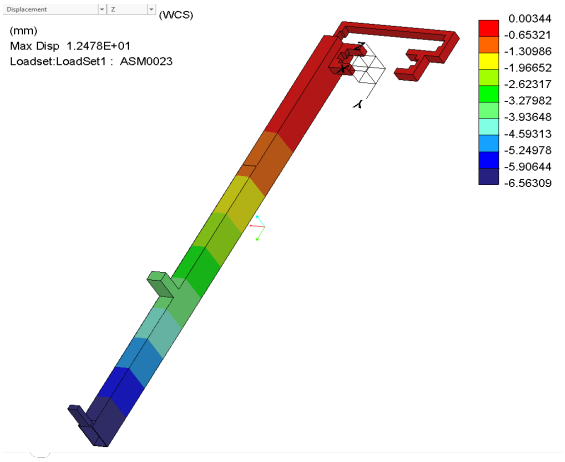

Figure 4.42: FEA assembly considering both loads with a maximum downward displacement of 6.58 mm.

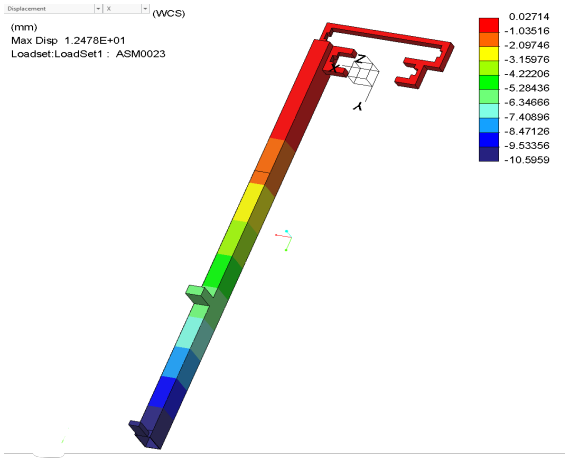

Figure 4.43: FEA assembly considering both loads with a maximum inward displacement of 10.59 mm.

In order to solve this issue, the sharp edges of the RHS are smoothed out, as shown in figures 4.44 and 4.45.

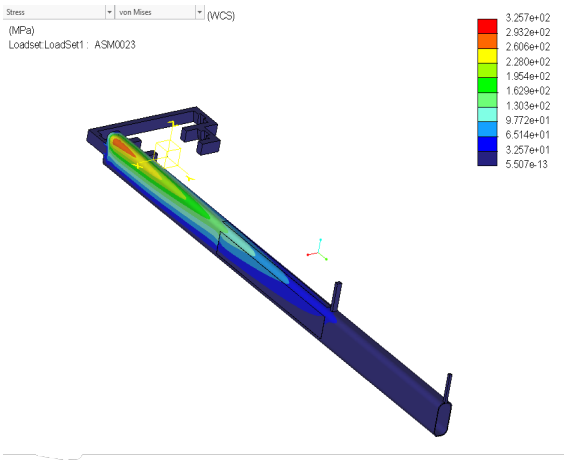

Figure 4.44: FEA assembly using both loads with a maximum Von Mises stress of 325, 7 MPa.

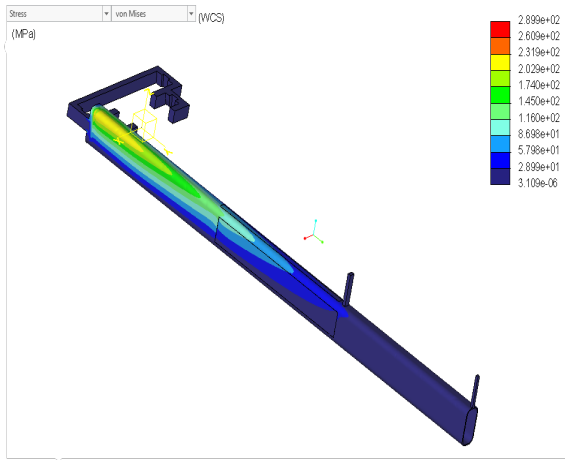

Figure 4.45: FEA assembly using both loads with a maximum Von Mises stress of 289, 9 MPa.

To further reduce the stress, the wall thickness was increased, which provided a decreased stress seen in figures 4.46 and 4.47.

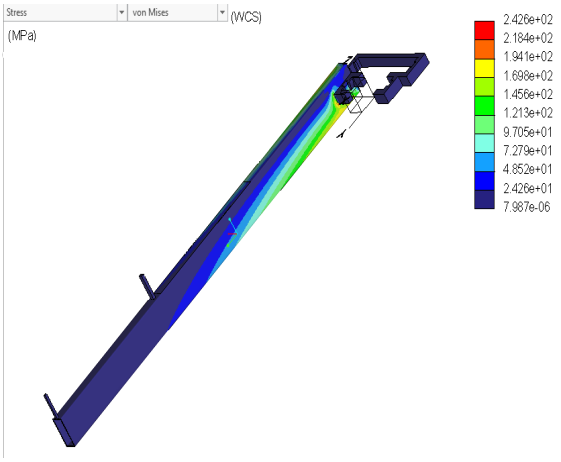

Figure 4.46: FEA assembly using both loads with a maximum Von Mises stress of 242, 6 MPa.

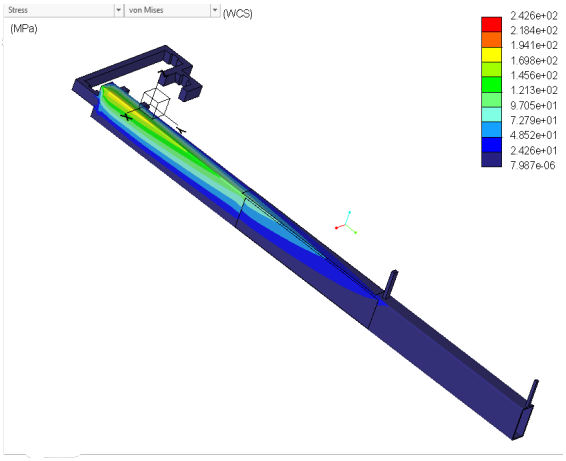

Figure 4.47: FEA assembly using both loads with a maximum Von Mises stress of 242, 6 MPa from another view.

After smoothing the sharp edges in the last iteration, a robust and mathematically validated solution is shown in figure 5.1.

Chapter 5

Results and Analysis

5.1 Final solution

The final concept weighs 6.33 kg and without the modular arms attached 4.55 kg. The arms consist of a cross-section 60x30x2 mm, which is shown in figure 5.1. The solution consists of two arms, one mounted permanently to the bracket and one additional arm that is detachable, depending on the dimensions of the pump.

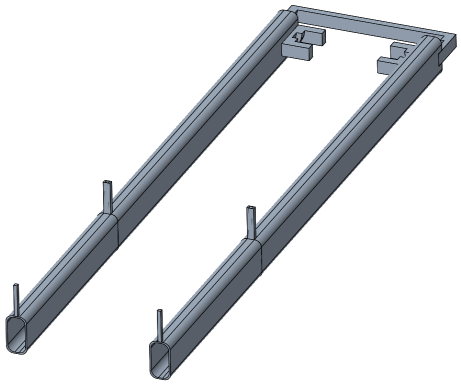

Figure 5.1: Front view of the final solution of the cable hook.

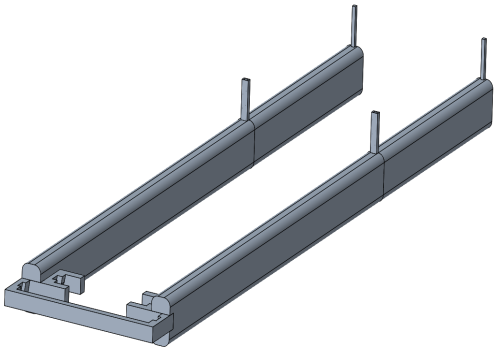

Figure 5.2: Back view of the final solution of the cable hook.

The bracket consists of two different tracks. The first track suits the largest lifting bracket, while the second track is adjusted for the two smaller lifting brackets. The second track has two different angles to fit both lifting brackets. The tracks are created by a Boolean operation with the cut function, so a solid part is first created and then inserted into an assembly where it is merged with the lifting brackets at the desired position, as visualized by the blue lines in figure 5.3. Then the function cuts out material and the tracks are created.

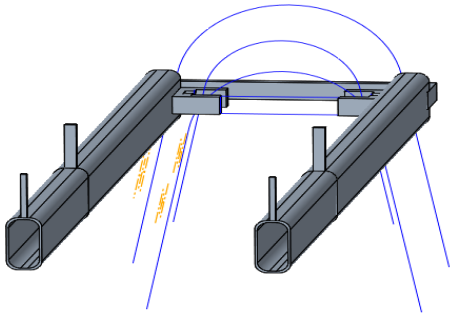

Figure 5.3: Front view with the cut out positions of the different lifting brackets in blue lines.

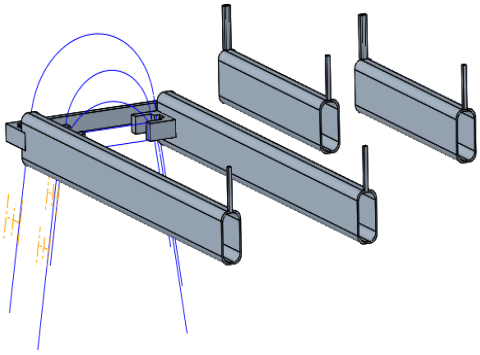

Figure 5.4: Exploded view of the solution.

5.1.1 Design of manufacture

The bracket will be manufactured from a thick plate using a multi-axis 3D waterjet cutting machine.

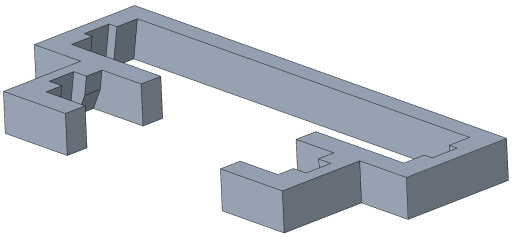

Figure 5.5: Attachment bracket to insert the lightning brackets into.

The main arm is constructed from a standard rectangular hollow section RHS. To create the mating surface, two thick plates will be welded inside the hollow section. The material between these welded plates will then be cut out to create a slot, allowing the arm to be inserted around the bracket. To mount the modular arm and prevent the cable from slipping, a smaller plate will be welded to the tip of the main arm.

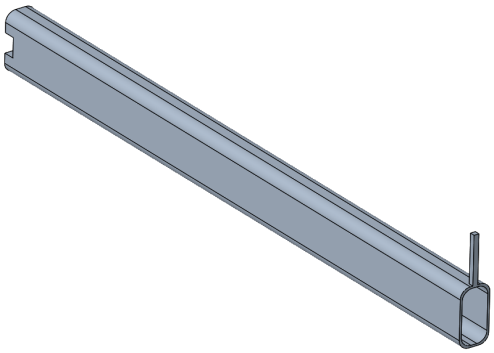

Figure 5.6: Front view of the arm.

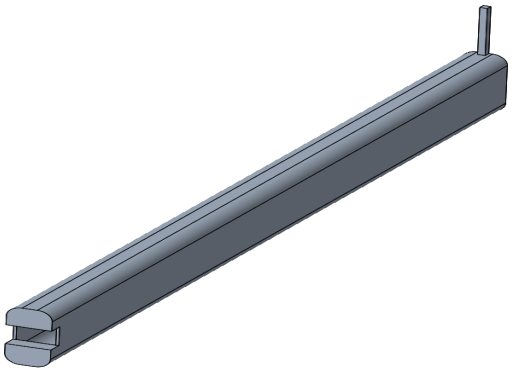

Figure 5.7: Back view of the arm.

The modular arm will be constructed from the same RHS. A mounting plate to connect it to the main arm and a tip to prevent cable slippage will be welded to this modular arm. The tip of the modular arm will match the profile of the hollow section, enabling further extension of the arms if necessary.

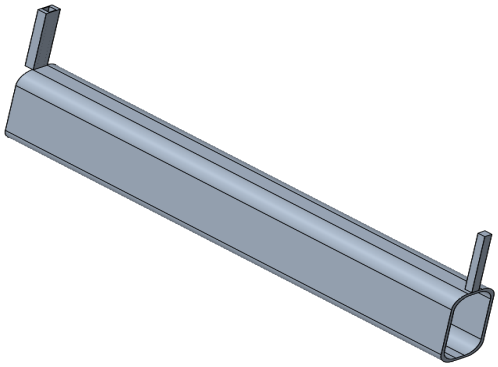

Figure 5.8: Front view of modular arm.

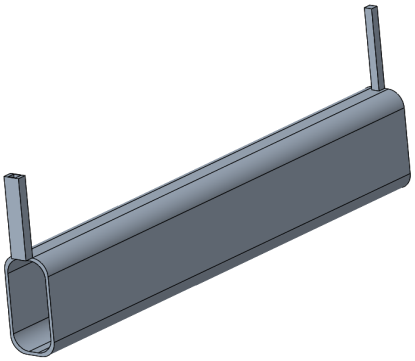

Figure 5.9: Back view of modular arm.

5.2 Simplified simulation

The highest stress will occur at the start of the arm due to the moment. A simplified simulation of only the arm and the module is used to create a more accurate and reliable simulation model. Since the solution generates forces along two axes, two iterative simulations are needed to ensure its strength. One case considers the vertical force, and another case includes the horizontal force. In order to avoid unture high stresses due to BC and sharp corners from the rectangular arm, the model had additional material applied to the structure at the start of the arm with a 10 mm thick plate.

5.3 Simulation of assembly

When considering all components and all forces simultaneously to create a more realistic model, the maximum stress due to the vertical force was 213.3 MPa.

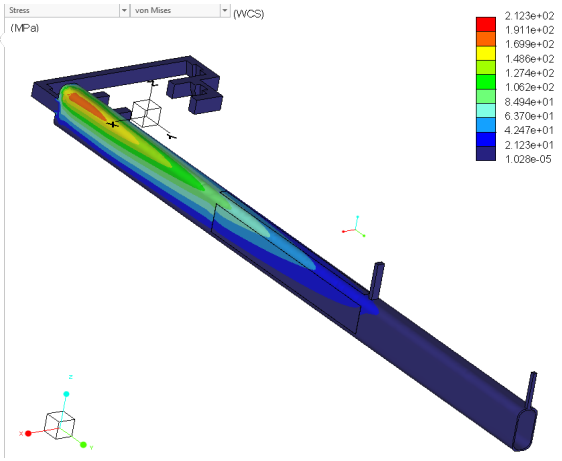

Figure 5.10: FEA assembly considering both forces with a maximum Von Mises stress of 213, 3 MPa.

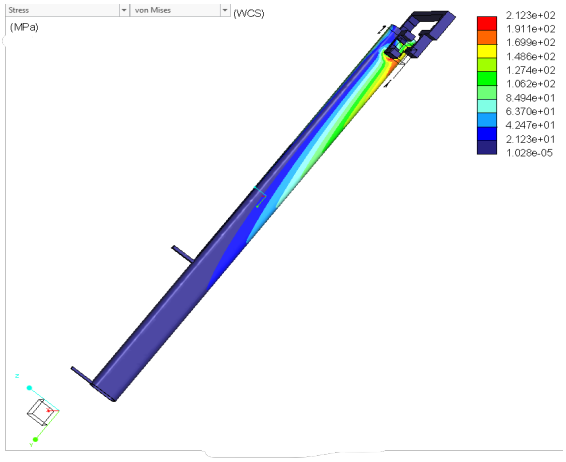

Figure 5.11: FEA assembly considering both forces with a maximum Von Mises stress of 213, 3 MPa from another view.

The maximum inward displacement is 7.68 mm and the downward displacement 4.73 mm.

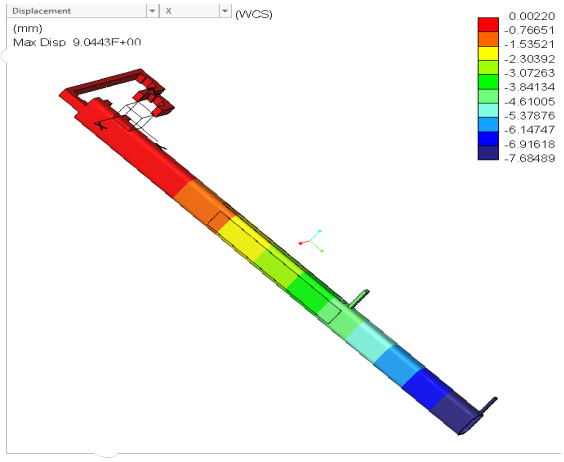

Figure 5.12: FEA assembly considering both loads with a maximum inward displacement of 7.58 mm.

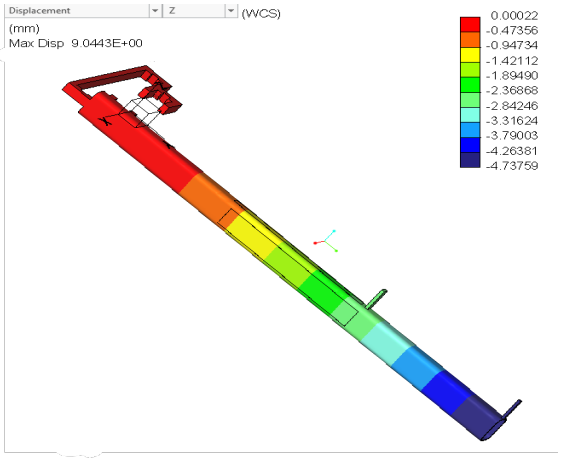

Figure 5.13: FEA assembly considering both loads with a maximum downward displacement of 4.73 mm.

5.4 Hand calculations

Analytical calculations are performed to ensure the reliability of the computational FE model. These are simplified versions with rougher assumptions for computational simplicity.

5.4.1 Beam deflection and maximum stress

Both arms are symmetric, which simplifies the model by allowing calculation of half the load on one arm. The total length of the arm is 951 millimeters and since the load

is distributed over two surfaces 300 millimeters adjacent to each other, the center of gravity occurs in the middle of these loads.

$$351 + 600/2 = 651 \text{ mm} \tag{5.1}$$

The worst cable case involves two cables weighing 100 kg each, which is then simplified into one case of 100 kg at both surfaces and gives a force of 981 newtons due to gravity. The moment is determined by force multiplied by distance as follows:

$$M_{\max} = 981 \text{ N} \cdot 0,651 \text{ m} = 638,6 \text{ Nm} = 638\,600 \text{ Nmm} \tag{5.2}$$

Since the beam is a hollow square tube, the moment of inertia is determined by the difference between the whole tube and the empty space as from [22]:

$$I = \frac{B \cdot H^3}{12} - \frac{b \cdot h^3}{12} \tag{5.3}$$

The maximum stress occurs at the furthest point from the force applied to the structure, which is at the merger of the attachment and the start of the arm. This is where the most moment occurs. The stress is calculated based on [22]:

$$\sigma = \frac{M \cdot e}{I} \tag{5.4}$$

Where e is the distance from the bending axis to the edge of the structure, which is in this case:

$$e = \frac{h}{2} \tag{5.5}$$

The load distribution is not applied to the whole beam, which is not a standard case [22]. To solve this, the superposition principle is applied, reducing the problem into two cases that are then added together.

1. Beam loaded with q over the entire length.
2. Subtracted with q on the unloaded part.

Based on the following data:

- Total length of beam (L): 951 mm
- Distribution of load (a): 600 mm (placed at the far end of the beam)
- Unloaded inner route (c): $L - a = 951 - 600 = 351$ mm
- Lever to the load's center of gravity (x): $c + \frac{a}{2} = 351 + 300 = 651$ mm
- Modulus of elasticity (E): 209 000 MPa (N/mm^2)
- Yield strength (S235): 235 MPa

5.4.1.1 Case 1: Force applied vertically

The beam is loaded vertically with 100 kg from above. The bending occurs over the strong axis of the cross-section, which is determined by the force multiplied by the distance to the middle of the distributed load.

$$F = 100 \cdot 9,81 = 981 \text{ N} \tag{5.6}$$

$$M_{max} = F \cdot x = 981 \cdot 651 \approx 638\,600 \text{ Nmm} \tag{5.7}$$

The second moment of inertia is determined by the difference between the outer cross-section and the inner cross-section [22]. The outer width is $B = 30$ mm and height $H = 60$ mm. Inner width is $b = 27,5$ mm and height $h = 57,5$ mm.

$$\begin{aligned} I &= \frac{30 \cdot 60^3}{12} - \frac{26 \cdot 56^3}{12} \\ I &\approx 159\,498 \text{ mm}^4 \end{aligned} \tag{5.8}$$

The maximum bending stress (σ) occurs at the tip of the distance from the neutral axis to the end of the cross-section [22], which is $y = H/2 = 30$. According to Navier's formula:

$$\begin{aligned} \sigma_{max} &= \frac{M_{max} \cdot y}{I} \\ \sigma_{max} &= \frac{638\,600 \cdot 30}{159\,498} \approx 120,1 \text{ MPa} \end{aligned} \tag{5.9}$$

This results in a safety factor of $235/120,1 \approx \mathbf{1,95}$, which provides safe construction against plasticization.

The deflection (δ) in the free end is determined by the superposition principle, which consists of the distributed load minus a fictitious load on the inner unloaded part. The distributed load is $q = 981/600 = 1,635$ N/mm.

$$\begin{aligned} \delta &= \frac{q \cdot L^4}{8 \cdot E \cdot I} - \left(\frac{q \cdot c^4}{8 \cdot E \cdot I} + \frac{q \cdot c^3}{6 \cdot E \cdot I} \cdot (L - c) \right) \\ \delta &= \frac{1,635 \cdot 951^4}{8 \cdot 209\,000 \cdot 159\,498} - \left(\frac{1,635 \cdot 351^4}{8 \cdot E \cdot I} + \frac{1,635 \cdot 351^3}{6 \cdot E \cdot I} \cdot 600 \right) \\ \delta &\approx 5,01 - (0,09 + 0,21) \approx 4,71 \text{ mm} \end{aligned} \tag{5.10}$$

5.4.1.2 Case 2: Force applied horizontally

The same principle applies as in case one, except that the beam is loaded with 55 kg from the side.

The force F and the maximum bending moment at the clamping force M_{max} are calculated:

$$F = 55 \cdot 9,81 = 539,55 \text{ N} \tag{5.11}$$

$$M_{max} = F \cdot x = 539,55 \cdot 651 \approx 351\,247 \text{ Nmm} \tag{5.12}$$

The second moment of inertia of a rectangular hole profile is with inverted height and width compared to case one:

$$\begin{aligned} I &= \frac{B \cdot H^3}{12} - \frac{b \cdot h^3}{12} \\ I &= \frac{60 \cdot 30^3}{12} - \frac{56 \cdot 26^3}{12} \\ I &\approx 52\,978 \text{ mm}^4 \end{aligned} \tag{5.13}$$

Maximum bending stress (σ) is determined by the distance from the neutral axis to the outermost fiber, which is now $y = H/2 = 15$ mm.

$$\begin{aligned} \sigma_{max} &= \frac{M_{max} \cdot y}{I} \\ \sigma_{max} &= \frac{351\,247 \cdot 15}{52\,978} \approx 99,45 \text{ MPa} \end{aligned} \tag{5.14}$$

The safety factor is $235/99 \approx \mathbf{2.37}$, which also lies within the safe margin prior to plasticization.

The deflection (δ) in the free end is determined by the superposition principle, which consists of the distributed load minus a fictitious load on the inner unloaded part. The distributed load is $q = 539,55/600 = 0,89925$ N/mm.

$$\begin{aligned} \delta &= \frac{q \cdot L^4}{8 \cdot E \cdot I} - \left(\frac{q \cdot c^4}{8 \cdot E \cdot I} + \frac{q \cdot c^3}{6 \cdot E \cdot I} \cdot (L - c) \right) \\ \delta &= \frac{0,89925 \cdot 951^4}{8 \cdot 209\,000 \cdot 52\,978} - \left(\frac{0,89925 \cdot 351^4}{8 \cdot E \cdot I} + \frac{0,89925 \cdot 351^3}{6 \cdot E \cdot I} \cdot 600 \right) \\ \delta &\approx 8,30 - (0,154 + 0,351) \approx 7,795 \text{ mm} \end{aligned} \tag{5.15}$$

5.4.2 Force distribution

Since the structure consists of two arms on which the cable will rest, an additional inward horizontal force will act on the arms. Since the normal force will be perpendicular to the contact surface, which is, in this case, at an angle to the horizontal plane. If a free-body diagram is constructed for one of the arms, the following forces act on the system.

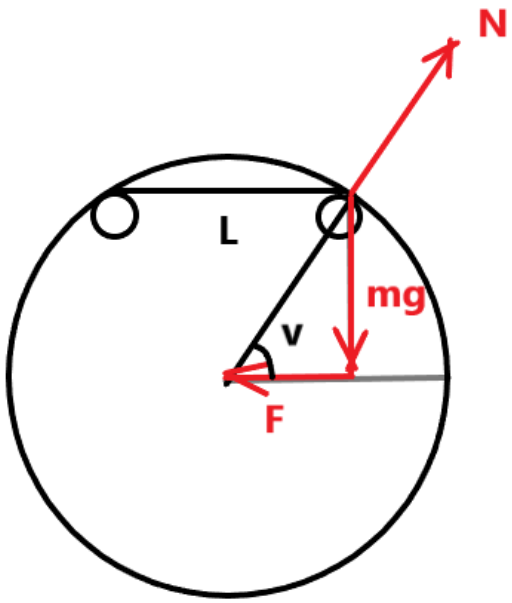

Figure 5.14: Free body diagram of cable placed on the arms.

The angle v is determined by trigonometry and the inward force by the gravitational force and tangents.

$$\varphi = \arccos\left(\frac{L/2}{R}\right) = \arccos\left(\frac{12}{R}\right) \tag{5.16}$$

The calculations are based on a 100 kg cable with an inner diameter of the rolled up cable $D = 50$ mm $\implies \varphi = 61,31°$

$$\begin{aligned} \tan\varphi &= \frac{mg}{F_H} \\ \implies F_H &= \frac{mg}{\tan\varphi} = \frac{981}{\tan(61,31°)} = 538,85 \text{ N} \end{aligned} \tag{5.17}$$

5.4.3 Pressure distribution in attachment

To determine how much force affects the attachment solution, a free-body diagram is constructed.

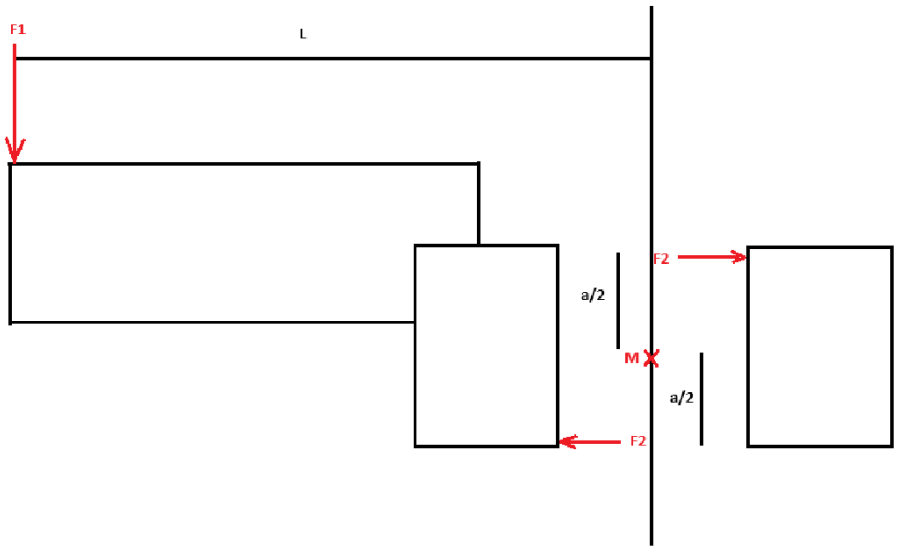

Figure 5.15: Free-body diagram of how the contact forces act on the attachment.

To determine the only unknown force F_2, a moment equation is performed based on point M.

$$\begin{aligned} \curvearrowleft \sum M: \quad & F_1 \cdot L = a \cdot F_2 \cdot \frac{1}{2} \cdot 2 \\ \implies & F_2 = \frac{F_1 \cdot L}{a} = \frac{1000 \cdot 651}{20} = 32\,550 \text{ N} \end{aligned} \tag{5.18}$$

The total contact force in both points is 32 550 N. Since the bracket of the cable holder needs to have free space for multiple layers of paint in order to fit the lifting brackets after multiple paintings iterations, it creates an infinitesimal contact surface that, in turn, creates a significant force impacting the lifting bracket at two points seen in figure 5.16 and in equation 5.19 [22].

Figure 5.16: The locking mechanism of the old solution between the lifting bracket and the bracket from the cable holder.

$$P = \frac{F}{A} \tag{5.19}$$

However, when the structure deforms or yields, the contact surface will increase until the stress drops to match the yield strength of the material. The force will then be distributed over a larger area, which in turn lowers the stresses and then stops the deformation.

5.5 Comparison analytic calculations and FEM simulation

Table 5.1: Comparison of Deflection and Stress Results

	Deflection δ (mm)		**Stress σ (MPa)**	
Model	**Horizontal**	**Vertical (z)**	**Horizontal**	**Vertical (z)**
Hand Calculations	11.69	7.20	149.05	183.60
Assembly Model	10.69	6.66	252.70	183.60

5.6 Physical prototype

The physical prototype had a total weight of 7.6 kg, where the arms consist of two different dimensions of the RHS profile in order to be able to move it back and forth to avoid disassembling for the smaller pumps. The construction has a stop function with an indexing bolt with a spring to adjust the arm length. It also has additional plates in order to be on the safe side to increase its robustness and additional distance between the arms to solve the problem with two cable connectors, which clash with the previous solution. The thickness of the RHS is also increased to improve manufacturability and facilitate welding.

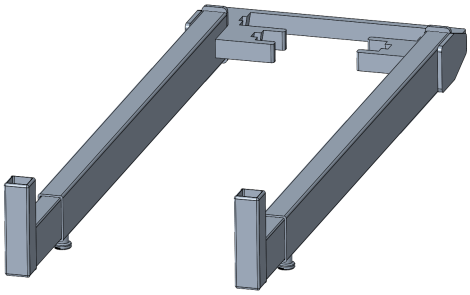

Figure 5.17: Front view of prototype concept in Creo.

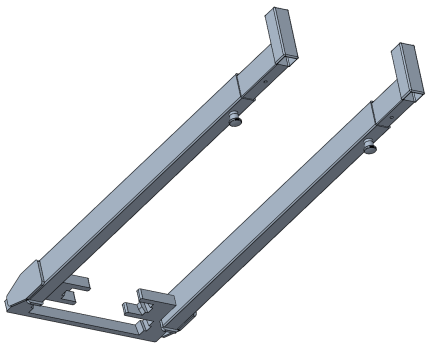

Figure 5.18: View from below of prototype concept in Creo.

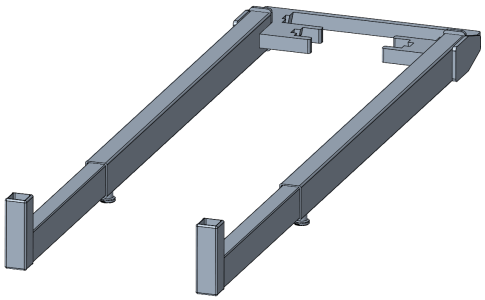

Figure 5.19: Front view of prototype concept with extended arms in Creo.

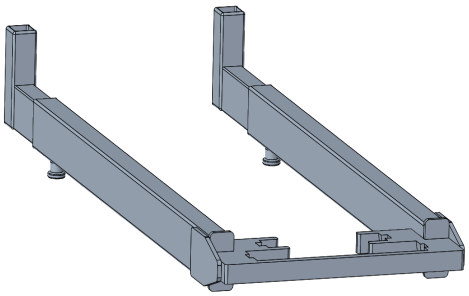

Figure 5.20: Back view of prototype concept in Creo.

In order to manufacture the prototype, the following drawing material was produced:

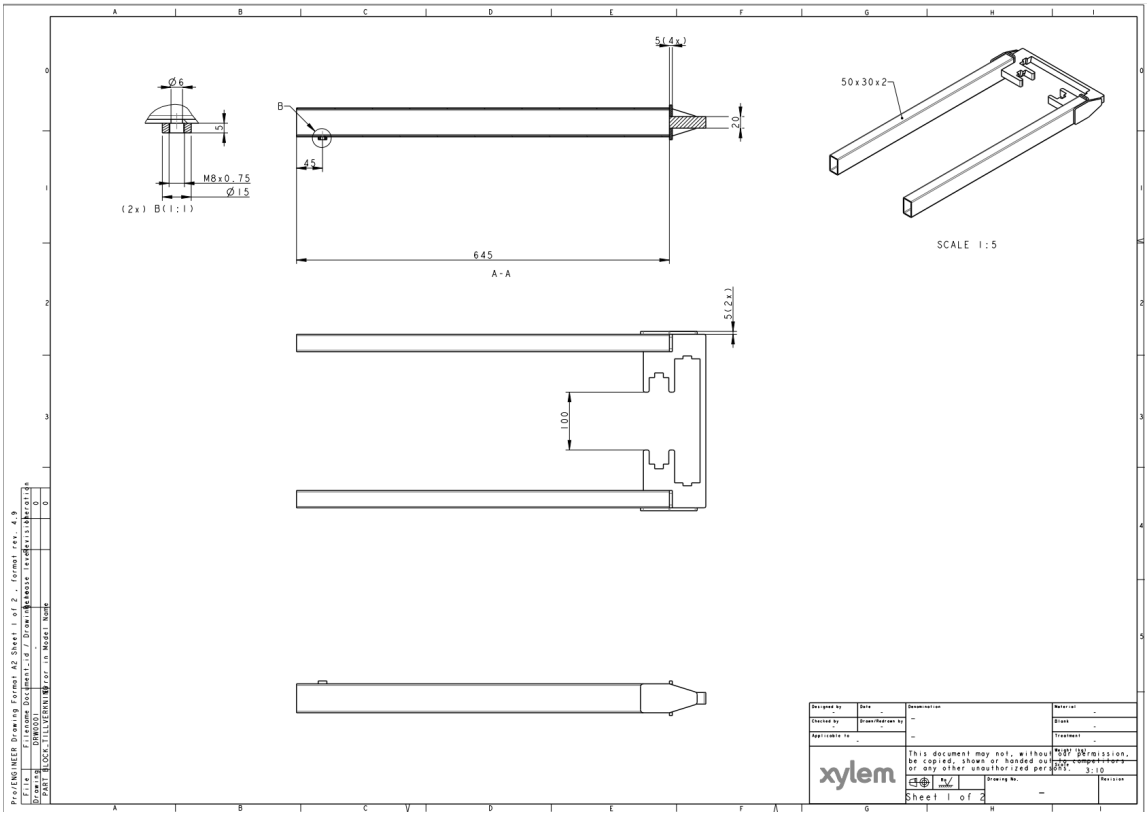

Figure 5.21: 2D drawing of the attachment and the arms merged.

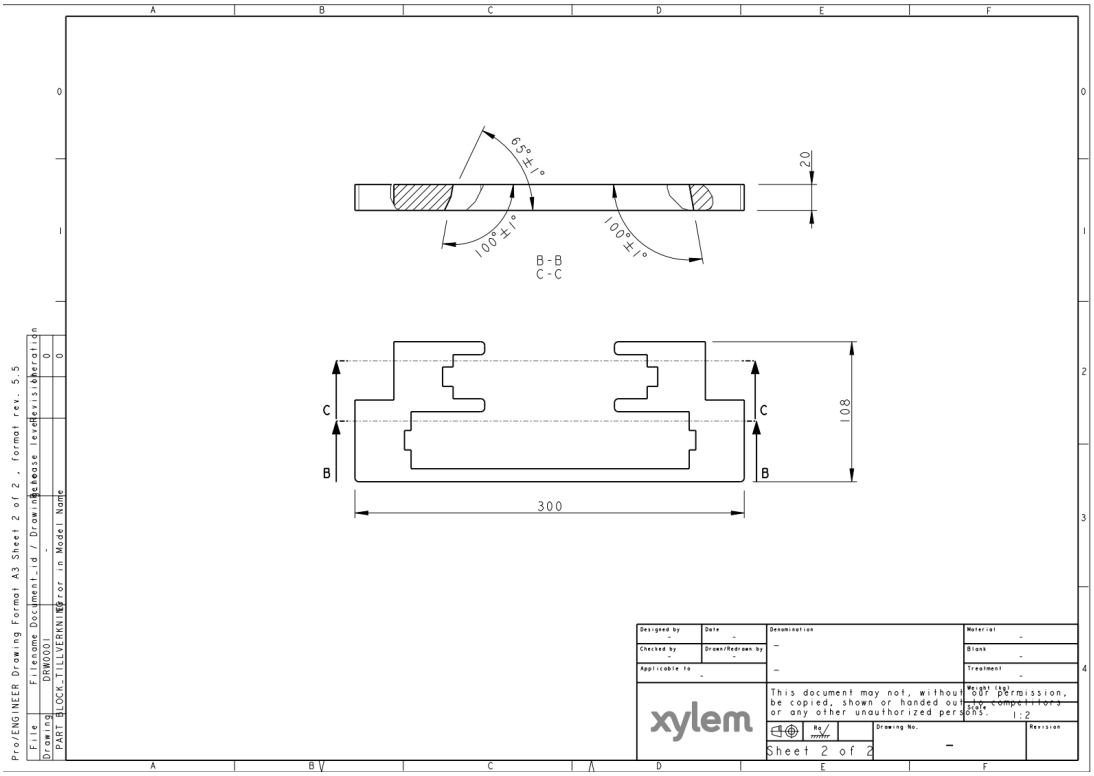

Figure 5.22: More detailed 2D drawing of the attachment.

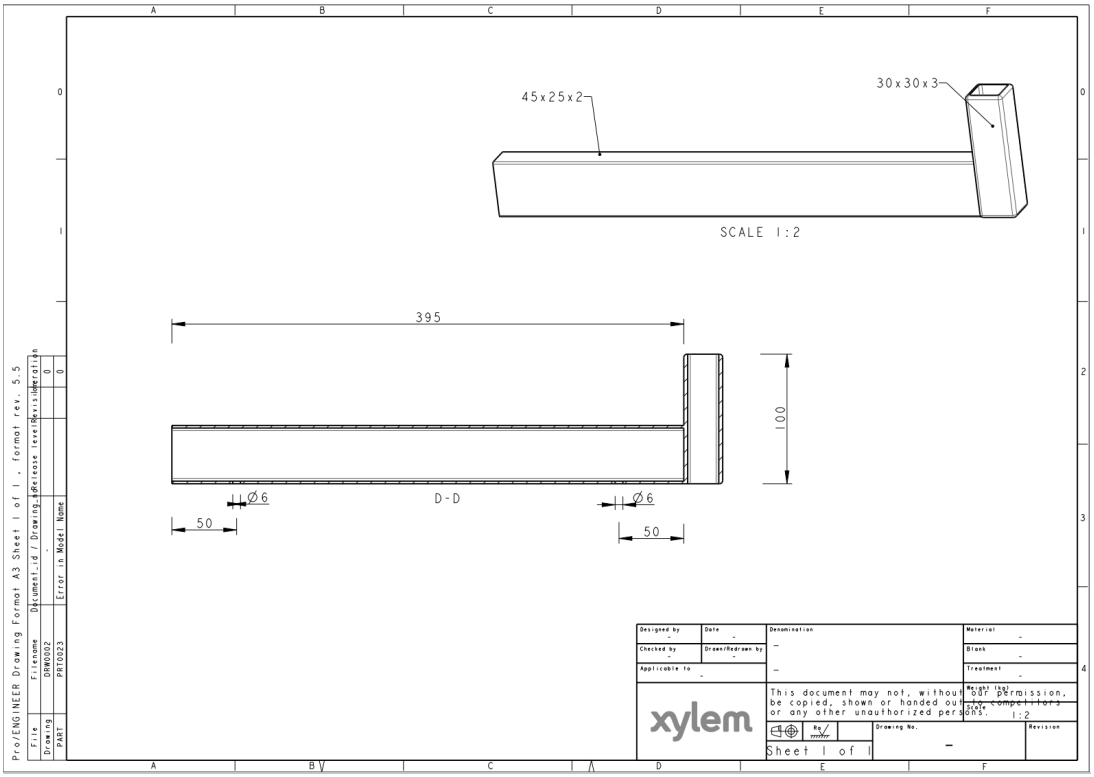

Figure 5.23: 2D drawing of the modular arm.

5.6.1 Analytic calculations of prototype

For the prototype, the same method is used as in the hand calculation part, with a 100 kg vertically and a 55 kg horizontally cable load is considered. For the 100 kg case:

Now with the outer width of $B = 30$ mm and height $H = 50$ mm. Inner width is $b = 26$ mm and height $h = 46$ mm.

$$\begin{aligned} I &= \frac{30 \cdot 50^3}{12} - \frac{26 \cdot 46^3}{12} \\ I &\approx 101\,605 \text{ mm}^4 \end{aligned} \tag{5.20}$$

The distance from the neutral axis to the end of the cross-section is $y = H/2 = 25$. According to Navier's formula:

$$\begin{aligned} \sigma_{max} &= \frac{M_{max} \cdot y}{I} \\ \sigma_{max} &= \frac{638\,600 \cdot 25}{101\,605} \approx 157,1 \text{ MPa} \end{aligned} \tag{5.21}$$

With a safety factor of $235/157,1 \approx \mathbf{1,50}$, which provides safe construction against plasticization.

The same principle applies with the 55 kg case from the side. The second moment of inertia of a rectangular hole profile is with inverted height and width compared to case one:

$$\begin{aligned} I &= \frac{B \cdot H^3}{12} - \frac{b \cdot h^3}{12} \\ I &= \frac{50 \cdot 30^3}{12} - \frac{46 \cdot 26^3}{12} \\ I &\approx 45\,125 \text{ mm}^4 \end{aligned} \tag{5.22}$$

Maximum bending stress (σ) is determined by the distance from the neutral axis to the outermost fiber, which is now $y = H/2 = 15$ mm.

$$\begin{aligned} \sigma_{max} &= \frac{M_{max} \cdot y}{I} \\ \sigma_{max} &= \frac{351\,247 \cdot 15}{45\,125} \approx 116,8 \text{ MPa} \end{aligned} \tag{5.23}$$

The safety factor is $235/116,8 \approx \mathbf{2,0}$, which is also within the safe margin of plasticization.

Chapter 6

Discussion

6.1 Takeaways from Concept Generation

In the early stages during the concept generation phase, the most opportunities were available. However, a generalization to meet all requirements from the alternating cases and still fulfill the customers' demands in terms of feasibility, costs and practicality led to a decrease in opportunities since trade-offs were constantly made. The balancing of cost, strength, and manufacturability mirrors the approach of weighted factors used by Manee-ngam et al. [7], where multiple design criteria are rated to identify a superior model.

Furthermore, customer uncertainty in the early stages of the process tends to lead to a more open solution that accommodates potential changes, thereby creating trade-offs. Every trade-off results in a less ideal solution for the affected requirements and the overall solution, so when multiple constraints and demands interact, the solution tends to converge toward a middle ground, optimized for this industrial scenario. On the other hand, the learning and approach of the iterative process of finding the ideal solution, in this case, similar to the iterative redesign and remodeling process described by Teke et al. [10], could be a useful tool and manual for implementing in other industrial cases.

The requirement of being able to hook the cable from the cable holder narrowed the scope of opportunities in the arm concept generation phase. For robustness, uniform structures are preferred when free space is required between the attachment of the cable, with limited opportunities for adding support in between. The required length of the arm to be able to paint the pump without disassembling the cable holder results in increased bending moments and thus increased stresses, which also result in higher material requirements.

Additionally, the cable holder is exposed to movements in multiple directions, which results in the attachment needing to be locked from only two of three directions and mountable from one direction. At the same time, it can not be dismounted in the production process without the impact of the production worker. Ensuring that these stress levels remain within the material's strength limits while reducing weight was also the primary objective in the TO study conducted by Hiep et al. [8].

6.2 Takeaways from the iterative Design- and Topology Optimization

The iterative design- and TO resulted in a weight reduction of 34% compared to the final solution and the heaviest cable holder of 9.6 kg, while the physical prototype showed a weight reduction of 20%. By making it more manufacturable, the weight increased by nearly 1.3 kg, which increased the weight of the final solution by 20%. This indicates that manufacturability and cost efficiency have a vital impact on the ability to reduce weight. This follows the economic part presented by Manee-ngam et al. [7], whose research demonstrated that optimized hook designs could achieve a 27.49% reduction in material costs while maintaining satisfying safety factors.

In order to achieve satisfactory results on iterative design- and TO the preparatory work is the most important part to obtain reliable and accurate results. If the BC is placed too close to exposed regions, such as sharp corners or regions of stress concentration, the stresses can rise to unrealistic levels. The BC issue is seen in the work of Teke et al. and Hiep et al. [8, 10]. These studies demonstrate successful weight reduction, while on the contrary, the results rely on the assumption of isolated and accurate BC. This makes the preparatory work of defining adequate BC and constraints the most critical part in avoiding insufficient results that do not reflect physical reality. Additionally, the challenge of managing these stress concentrations is similar to the work of Holmberg et al. [9], who used stress-constrained formulations to avoid failures in areas where traditional stiffness-based methods often fail.

Furthermore, it is important to create a clear overview of the possible impacts the structure will face. Otherwise, the realization of physical phenomena could occur later in the iterative process, resulting in increased design costs since adjustments need to be made and using less time for the right path. A clear example of this is the realization of the inward force created when visualizing the forces acting on the cable holder in a free-body diagram. The issue could not be solved while using the same concepts from the iterative design process, instead a new solution needed to be produced. The knowledge obtained from the iterative process provided the required dimensions to obtain a robust structure under the given loads. This made the next iterative process much faster in achieving satisfactory results and getting the final solution.

The research questions of the thesis are related to the iterative process of TO and are the following:

- What is the optimized geometry of the lifting solution using topology optimization, considering minimizing the Von Mises stresses and material consumption under different loads?
- How can results from topology optimization be used to develop a solution that considers different types of cargo?

Where the thesis has the following hypothesis:

- The most exposed parts, where critical stresses occurs needs more material. In regions with negligible stress, the material distribution will be reduced.

- The design of the attachment solution will include additional material at approximately the same locations for different loads. The noticeable difference should be in the amount of material required to apply.

Iterative attempts to reinforce the root by adding height at the locations of the critical stresses only moved the stress concentrations further along the arm. This led to increasing the vertical height and tapering of the profile being the most efficient procedures to maximize strength and reduce weight. This behavior aligns with Euler beam theory, where the bending strength and stiffness of a rectangular cross-section increase linearly in relation to its width. Doubling the width yields twice the strength, whereas doubling the height yields eight times the strength. Since calculating the second moment of inertia, the height is raised to the power of three, while the width is classified as a constant [22]. The iterative process also yielded a geometry resembling an I-beam, which is the most optimal solution for absorbing vertical forces. The iterative simulation process indicates that the material situated along the horizontal neutral axis experiences negligible stress. The cutouts based on the generative TO reveal the structurally negligible mass, where the upper and lower parts are preserved to handle the critical tensile and compressive stresses, which shows the possibility of weight reduction in generative TO. Although when the inward force was considered, the solution tended back to basic structures to withstand multi-axial loads, where the second moment of inertia needs to be fulfilled in both the horizontal and vertical directions.

The realization that vertical height and profile tapering were the most efficient procedures for maximizing strength validates the importance of the preparatory analytical work. This behavior is mathematically grounded in the cubic relationship between height and stiffness in rectangular cross-sections. Such findings complement the work of Holmberg et al. [9], particularly regarding their development of stress constrained optimization. Their research suggests that traditional methods often fail at stress concentrations. Similarly, this study found that without manual intervention of the geometrical strategy direction, the iterative TO process struggled to resolve peak stresses at the attachment root. The intervention of replacing the constraints solved the issue with the peak stresses. Moreover, the transition to a hollow rectangular structure was not a regression in design, but a necessary optimization to satisfy both the vertical stiffness requirements and the horizontal forces identified in the free-body diagram, while maintaining the cable holder at the lowest possible weight. The shift toward a more robust, multi-axial structure highlights a critical distinction between this thesis and the results presented by Manee-ngam et al. and Teke et al. [7, 10]. While both studies achieved significant weight reductions up to 27% by optimizing standard hooks, their models primarily focused on predictable, unidirectional loading at the hook's saddle. In contrast, the realization of the inward forces in this thesis required a balance of both horizontal and vertical stiffness. While the optimized results in the related studies demonstrate the high potential of TO under ideal conditions, this investigation reveals its limitations when facing the complex, uncertain load application points common in industrial environments. Under these multi-axial load cases, the usual mass reduction seen in simpler hook designs becomes less viable. In this case, additional material was applied to ensure horizontal structural integrity.

Other beam alternative was considered, such as I- and C-beams, but due to additional material requirements at the attachment in order to merge the beam with the block, made the attachment solution not economically justifiable to manufacture due to its new complexity. In this case, the attachment block has multiple height levels rather than a single height, which requires more operational steps to create. The marginal weight savings do not justify the added manufacturing complexity. The results in the thesis provide a counter-argument to Hiep et al. [8], who suggest that TO is economically efficient. Hiep et al. utilized 3D-printed ABS plastic, which offers great opportunities for geometric complexity. This study addresses industrial scalability, where a large number of cable holders are needed in production. If a purely TO result is manufactured, there is a high risk of increased production costs due to complexity in geometry, which consequently requires expensive welding, unique manufacturing setups and mirrored part requirements. Thus, TO saves material mass, the suboptimal rectangular pipe remains more economically justifiable when considering the total cost of production and assembly. From a production standpoint, the material required to realize the cable holder using causal I- and C-beams is not economically viable, as the increased assembly difficulty outweighs the minimal mass reduction. Furthermore, in the case of the C-beam, the need for mirrored left and right versions further increases production costs. Each version requires unique manufacturing steps and setups, leading to increased cost compared to a symmetrical design. Mounting the beams with only side bolts simplifies assembly but creates structural risks. The thin walls may crush when the bolts are tightened. Also, because the weight rests on a single thin wall, it creates high stress around the holes, which could lead to failure. For the C-beam, this side-mount makes its natural lack of stiffness, likely causing the beam to twist or warp under load.

6.3 Industrial contribution

The industrial contribution of this thesis is the development of a generalized, TO cable holder that balances weight reduction with manufacturing simplicity. In an industrial environment where requirements are often not fully established and are uncertain, creating a generalized design provides significant strategic advantages. Agility under uncertainty ensures that the optimized design is robust enough to handle varying loads or changes in demand from the customer. For the company, this means they do not need to re-engineer the cable holder for minor changes in requirements, saving engineering hours and money. The TO also reduces the need for prototyping and experimentation, thereby saving time and costs in prototype production. This aligns with the findings of Hiep et al. [8], who concluded that TO is a tool that optimizes not only material volume but also development time. By standardizing the use of multiple cable holders into a single optimized design, the company can drastically reduce its total inventory volume. Maintaining a single article number instead of several variations frees up administrative work, increasing traceability and workflow efficiency. Furthermore, the reduction in manufacturing steps and the avoidance of complex assembly operations result in lower unit costs. This relates to the consideration of economics presented by Manee-ngam et al. [7]. However, while their study focuses primarily on direct material savings, this thesis

expands that contribution to include manufacturability and other economic factors, such as reduced inventory management and simplified operational steps, for instance, avoiding complex water-cutting for the multi-level bracket.

Furthermore, when only one type of cable holder exists, the risk of an operator selecting the wrong component for a specific load case is eliminated. This ensures that the safety margins calculated during the TO process are always maintained in practice.

The TO process extends beyond the company's internal benefits, achieving societal and environmental goals. Reducing the material volume directly lowers the carbon footprint associated with steel production, which has a positive environmental impact, as less raw material requires less energy consumption during the manufacturing of the cable holders. There are also economic factors, since mass production becomes significantly more viable when parts are mirrored, requiring only one arm type and a modular part. Furthermore, the reduction in manufacturing steps and the avoidance of complex assembly operations result in lower unit costs, for instance, the water-cutting process of the attachment with multiple height levels. From an ethical standpoint, ensuring structural integrity through rigorous calculations rather than guesswork guarantees a safer working environment for end users, who rely on this cable holder to secure cargo. This study is of public interest for various actors within the transport and industrial sector, who need to transport cargo using hooks or attachment solutions for securing the cargo, especially where the distribution of the forces varies and is uncertain. Through simple benchmarking, this could be identified as a common problem in an industrial environment.

Chapter 7

Conclusions and Future Work

7.1 Conclusions

The iterative process of TO in this thesis revealed a fundamental truth in structural engineering, where computational optimization often converges toward traditional geometric solutions. While TO has the potential to generate complex shapes, the results of this study consistently pointed toward the efficiency of the RHS. This convergence validates that traditional profiles are not merely conventions but are reliable structures for handling multidirectional loads.

A critical turning point in this research was the realization that maximum weight savings do not equate to maximum value return. The early iterations of the design process focused solely on reducing the mass of a structure similar to an I-beam, which proved impractical when considering the entire manufacturing ecosystem. Initial attempts to use profiles similar to an I-beam required complex internal reinforcements and mirrored parts to mount the arm to the bracket. The added labor and complexity in creating the bracket rendered the theoretical weight savings economically unviable. In industrial reality, profitability is determined by the simplicity of the assembly line, not just by the component's lightness. If this thesis were conducted again, the approach would shift from first prioritizing manufacturing feasibility over optimization. Additionally, manufacturing constraints such as tool access and standard profile availability would be considered in the TO process from the first iteration, instead of only being considered at the end. In addition, the OF would not only minimize volume and stress but also include a complexity penalty system to favor designs that are easier to produce. Furthermore, the wrong turn taken during the design phase highlights the importance of early validation to catch integration issues, such as missing forces, before committing to a final geometry of rapid prototyping. The study concludes that the 2 mm RHS profile is the superior choice for the generalized cable hook, when considering multi-axis load cases. It represents the golden mean where the mathematical ideals of TO meet the hard requirements of industrial production. Ultimately, the most successful design is not the one that removes the most material, but the one that provides the highest structural safety and operational simplicity at the lowest total cost. To summarize, the design process in the end comes down to cost, manufacturability, and overall profitability.

7.2 Future work

This thesis provides a foundational framework for a generalized TO lifting solution. Several avenues for further research and development remain. A primary area for future investigation is whether a multi-standardization strategy would outperform a single universal design. It would be valuable to analyze whether introducing two distinct cable holders would yield enough material savings and possibly reduced costs to outweigh the added logistical complexity. A comparative study could quantify the break-even point between manufacturing simplicity and weight performance. This could be achieved by designing a specialized cable holder for loads under 50 kg and a reinforced version for loads exceeding 50 kg.

Future iterations should focus on the load-securing mechanism. The current design relies on the loads acting on the cable holder rather than on how the load will affect the securing mechanism. Furthermore, future work is needed to ensure greater stability during transport. This includes physical testing and investigation of dynamic stability during transport. Lastly, the locking mechanisms between the arm and the modular arm need analysis. Also, the development of a locking mechanism that secures the cargo more robustly against vibrations or incorrectly loaded cargo.

The interface between the mounting bracket and the lifting bracket remains a region of uncertain stress concentration. These stresses could be investigated experimentally by observing how deformations affect stress concentrations. Furthermore, further TO of the bracket's interface to reduce peak Von Mises stresses.

The current solution is optimized based on prototype manufacturing and standard profiles. To increase industrial profitability, the design should be investigated for high-volume production. This includes design for manufacturing, investigating more cost-effective manufacturing methods, for instance, automated welding, stamping, or casting, if volumes justify the tooling costs. Additionally, a financial study could be conducted comparing the generalized approach with multiple cable holders over a long-term production cycle, accounting for tool wear, assembly time, and material waste. Lastly, future research could include an FEA analysis of dynamic loads, as production workers are not careful with the equipment, tossing it around and stacking the cable holders on pallets carelessly.

References

[1] Ansys Inc., "What is Finite Element Analysis (FEA)? | Ansys." Ansys.com, Available: `https://www.ansys.com/simulation-topics/what-is-finite-element-analysis`. [Accessed: Apr. 17, 2026].

[2] G. Broman, *Computational Engineering*. Karlskrona: Avdelningen för maskinteknik, Blekinge tekniska högskola, 2003.

[3] J. R. R. A. Martins and A. Ning, *Engineering design optimization*. Cambridge: Cambridge University Press, 2022.

[4] Ansys Inc., "What is Topology Optimization? | Ansys." Ansys.com, Available: `https://www.ansys.com/simulation-topics/what-is-topology-optimization`. [Accessed: Apr. 17, 2026].

[5] J. S. Arora, *Optimization of structural and mechanical systems*. Hackensack, NJ: World Scientific, 2007.

[6] O. Sigmund and K. Maute, "Topology optimization approaches: A comparative review," *Structural and Multidisciplinary Optimization*, vol. 48, pp. 1031–1055, Dec. 2013.

[7] A. Manee-ngam, P. Saisirirat, and P. Suwankan, "Hook Design Loading by The Optimization Method With Weighted Factors Rating Method," *Energy Procedia*, vol. 138, pp. 337–342, Oct. 2017.

[8] V. D. Hiep, N. X. Quynh, and T. T. Tung, "A topology optimization design of a crane hook," *Results in Engineering*, vol. 23, p. 102492, Sept. 2024.

[9] E. Holmberg, B. Torstenfelt, and A. Klarbring, "Stress constrained topology optimization," *Structural and Multidisciplinary Optimization*, vol. 48, pp. 33–47, July 2013.

[10] I. T. Teke, M. Akbulut, and A. H. Ertas, "Topology optimization and fatigue analysis of a lifting hook," *Procedia Structural Integrity*, vol. 33, pp. 75–83, 2021.

[11] P. Johannesson and E. Perjons, *An Introduction to Design Science*. Springer eBook Collection, Cham: Springer International Publishing, 2nd ed. 2021 ed., 2021.

[12] K. Peffers, T. Tuunanen, M. A. Rothenberger, and S. Chatterjee, "A Design Science Research Methodology for Information Systems Research," *Journal of Management Information Systems*, vol. 24, pp. 45–77, Dec. 2007.

[13] B.-S. Kim, B. Shah, T. He, and K.-I. Kim, "A survey on analytical models for dynamic resource management in wireless body area networks," *Ad Hoc Networks*, vol. 135, p. 102936, Oct. 2022.

[14] J. Hou, G. Chen, J. Huang, Y. Qiao, L. Xiong, F. Wen, A. Knoll, and C. Jiang, "Large-Scale Vehicle Platooning: Advances and Challenges in Scheduling and Planning Techniques," *Engineering*, vol. 28, pp. 26–48, Sept. 2023.

[15] K. M. Meiburger, U. R. Acharya, and F. Molinari, "Automated localization and segmentation techniques for B-mode ultrasound images: A review," *Computers in Biology and Medicine*, vol. 92, pp. 210–235, Jan. 2018.

[16] I. Bouchrika, "What Is Empirical Research? Definition, Types & Samples for 2026." Research.com, Mar. 19, 2026. [Online]. Available: `https://research.com/research/what-is-empirical-research`. [Accessed: Apr. 17, 2026].

[17] PTC Inc., "To Set Convergence for a Structural Analysis." ptc.com, Available: `https://support.ptc.com/help/creo/creo_pma/r12/usascii/index.html#page/simulate/simulate/convergence.html`. [Accessed: Apr. 17, 2026].

[18] PTC Inc., "Multi-Pass Adaptive Convergence Method." ptc.com, Available: `https://support.ptc.com/help/creo/creo_pma/r12/korean/index.html#page/simulate/simulate/stat_multiadap.html`. [Accessed: Apr. 17, 2026].

[19] PTC Inc., "Convergence Quantity for Static, Prestress Static, Large Deformation, and Contact Analyses." ptc.com, Available: `https://support.ptc.com/help/creo/creo_pma/r12/chinese_tw/index.html#page/simulate/simulate/stat_convqty.html`. [Accessed: Apr. 17, 2026].

[20] TSD Engineering, "Multi-Pass Adaptive Convergence - TSD Engineering." ptc.com, Available: `https://www.woodgaswizard.com/tips-and-tricks/solution-convergence/multi-pass-adaptive-convergence/`. [Accessed: Apr. 17, 2026].

[21] H. MA, Y. MEI, D. MARMYSH, and S. JI, *Mechanics of Materials*. EDP Sciences, 2024.

[22] K. Björk, *Formler och tabeller för mekanisk konstruktion*, vol. 9. Karl Björks Förlag HB, 2011.

Appendix A

Supplemental Information

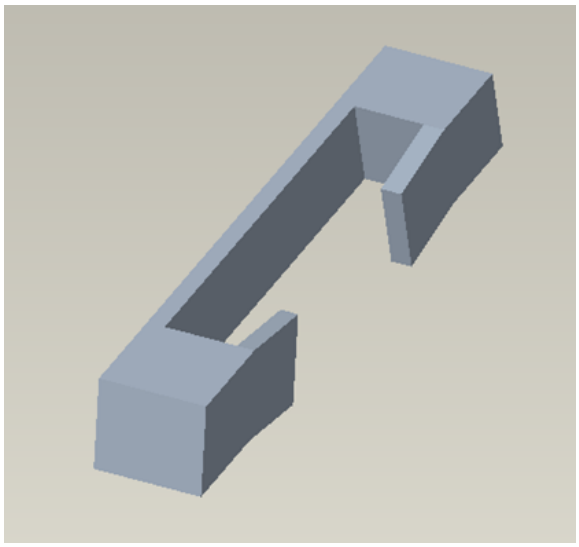

Figure A.1: Initial concept.

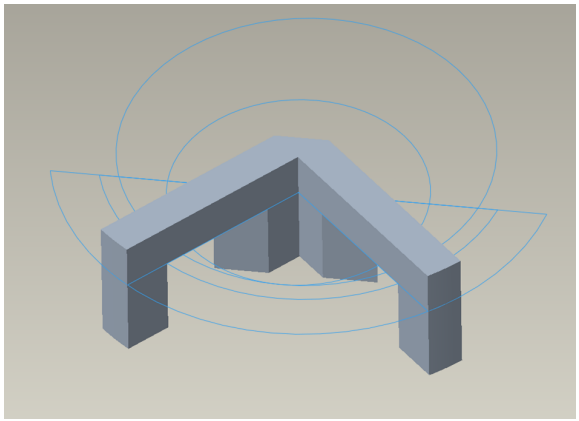

Figure A.2: Second concept.

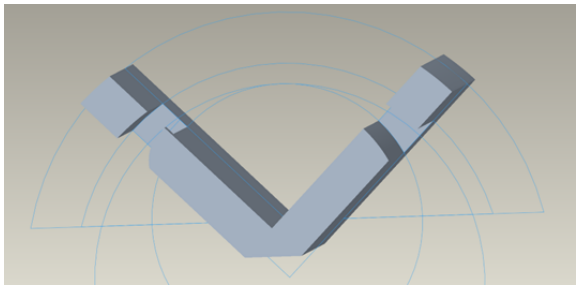

Figure A.3: Third concept.

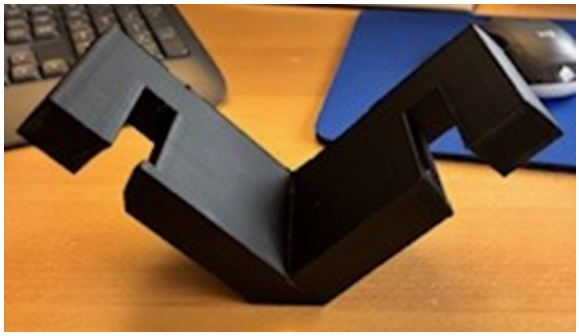

Figure A.4: Actual 3D-printed prototype of third concept.

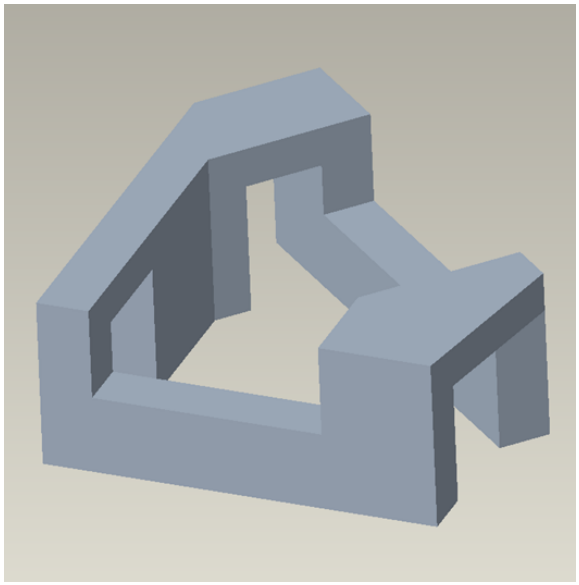

Figure A.5: Fourth concept.

Figure A.6: Actual 3D-printed prototype of fourth concept.

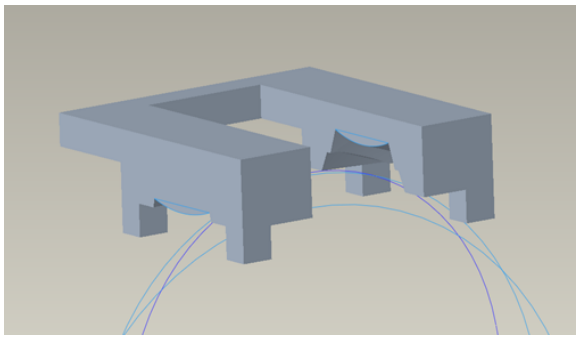

Figure A.7: Fifth concept.

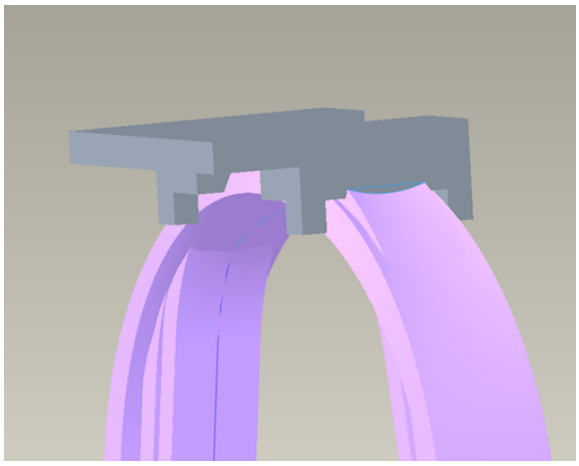

Figure A.8: Visual representation of the fifth concept applied on the lifting brackets.

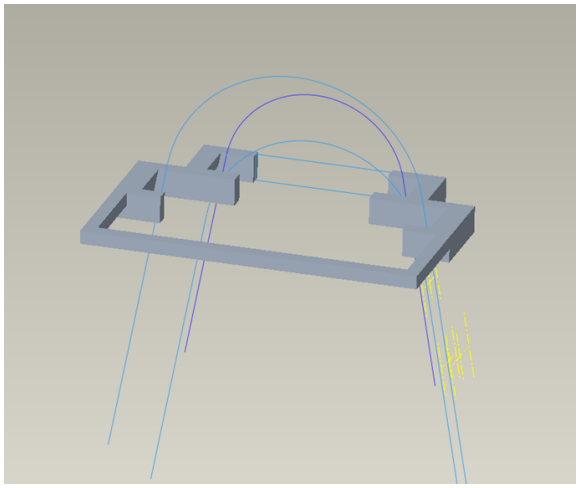

Figure A.9: Sixth concept.

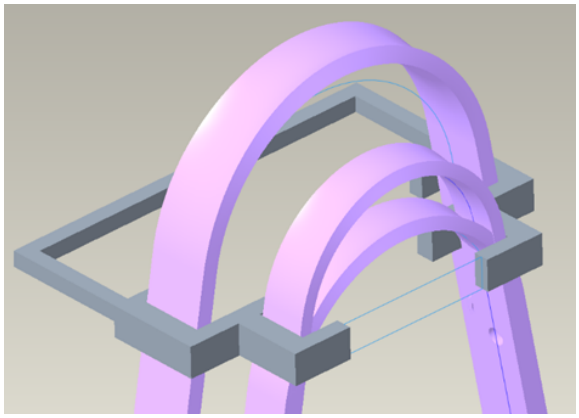

Figure A.10: Visual representation of the sixth concept applied on the lifting brackets.

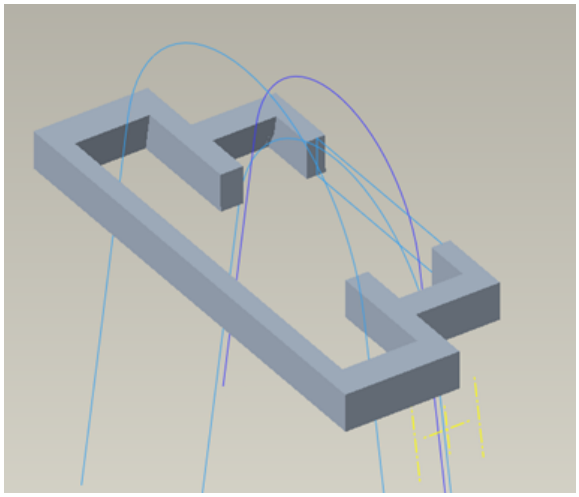

Figure A.11: Final concept.

Faculty of Engineering, Blekinge Institute of Technology, 371 79 Karlskrona, Sweden